Nuclotron based Ion Colider fAcility

Experimental opportunities for new physics at Nuclotron-NICA?

Arkadiy Taranenko (NRNU MEPhI)

International Conference on Quantum Field Theory, High-Energy Physics, and Cosmology, JINR, Dubna, 18-21 July, 2022

In collaboration with

- ✓ Petr Parfenov
- ✓ Alexander Demanov
- ✓ Mikhail Mamaev
- ✓ Ilya Segal
- ✓ Dim Idrisov
- ✓ Valery Troshin
- ✓ Oleg Golosov
- ✓ Ba Vinh Luong

Analysis of data from STAR(RHIC), NA61/SHINE(CERN), HADES(SIS18) HIC experiments

Performance for Flow Measurements with BM@N and MPD experiments at Nuclotron-NICA

NICA Accelerator Complex

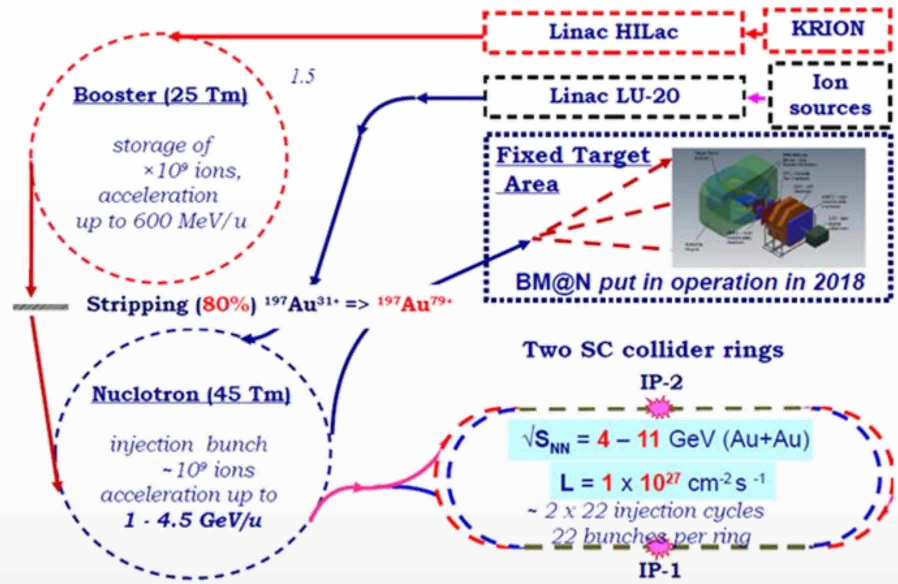

❖ Expected beam configuration in Stage-I:

✓ without electron cooling in collider, with stochastic cooling, reduced number of RFs → not-optimal beam optics

✓ reduced luminosity (~10^{25} is the goal for 2023) → collision rate ~ 50 Hz

✓ collision systems available with the current sources: C (A=12), N (A=14), Ar (A=40), Fe (A=56), Kr (A=78-86), Xe (A=124-134), Bi (A=209) → **start with Bi+Bi @ 9.2 GeV in 2023**, Au+Au @ 4-11 GeV to come later

Schedule of the MPD-NICA is significantly affected by the current geopolitical situation (suspension of collaboration with CERN and Polish & Czech Republic member institutions, economical sanctions and problems with supplies of many components from western companies). The primary goal to have the MPD commissioned by the first beams at NICA collider is preserved.

Multi-Purpose Detector (NICA)

Stage- I

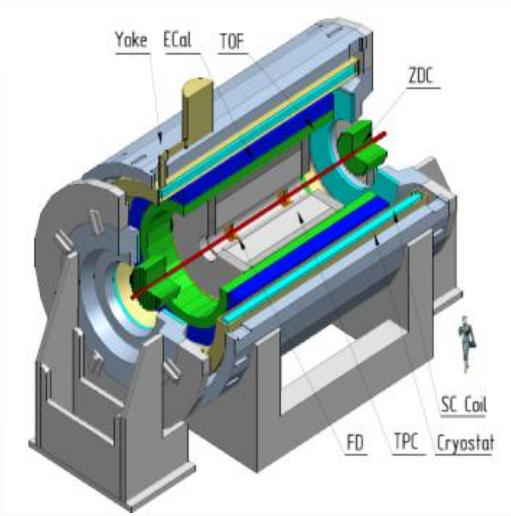

Length	340 cm
Vessel outer radius	140 cm
Vessel inner radius	27 cm
Default magnetic field	0.5 T
Drift gas mixture	90% Ar+10% CH_4
Maximum event rate	7 kHz ($L = 10^{27}$ $cm^{-2}s^{-1}$)

upgrade

($\sqrt{s_{NN}}$ = 4-11 GeV)

Stage- II

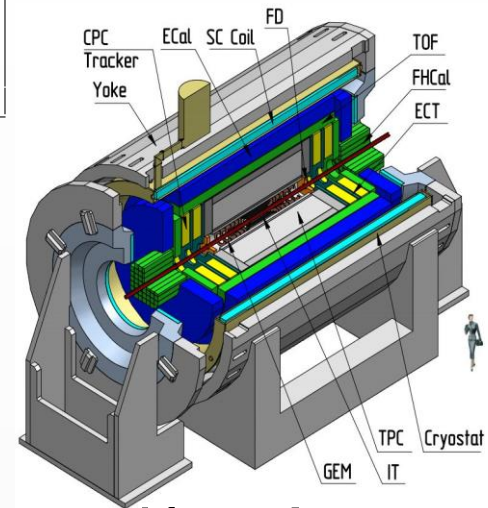

+ ITS and **forward spectrometers**

TPC: |Δφ| < 2π, |η| ≤ 1.6

TOF, EMC: |Δφ| < 2π, |η| ≤ 1.4

FFD: |Δφ| < 2π, 2.9 < |η| < 3.3

FHCAL: |Δφ| < 2π, 2 < |η| < 5

2024?: first run with Bi+Bi @ 9.2 GeV with luminosity ~ 10^{25} $cm^{-2}s^{-1}$

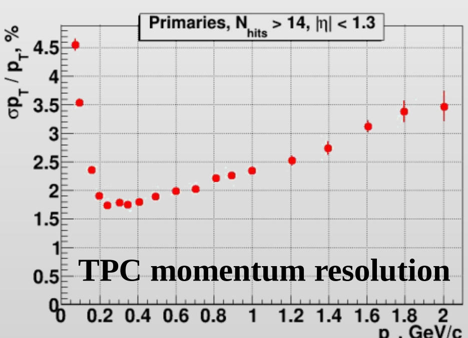

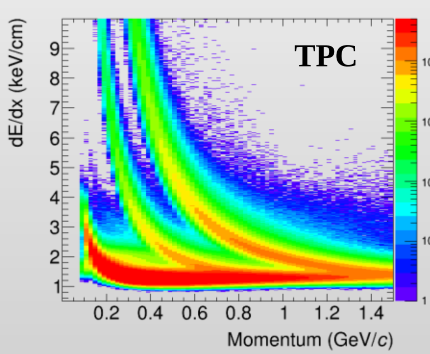

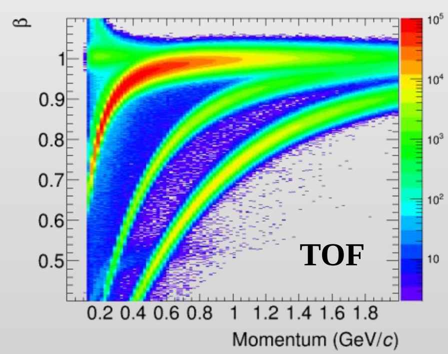

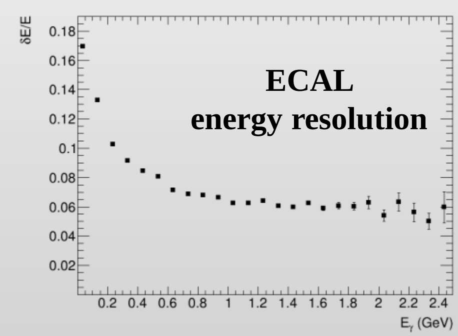

Reconstruction of hypertritons (MPD)

- Information on YN interactions, strange sector of nuclear EoS, astrophysics
- BiBi@9.2 GeV (PHQMD), 40 M sampled events:

Phys.Part.Nucl.Lett. 19 (2022) 1, 46-53

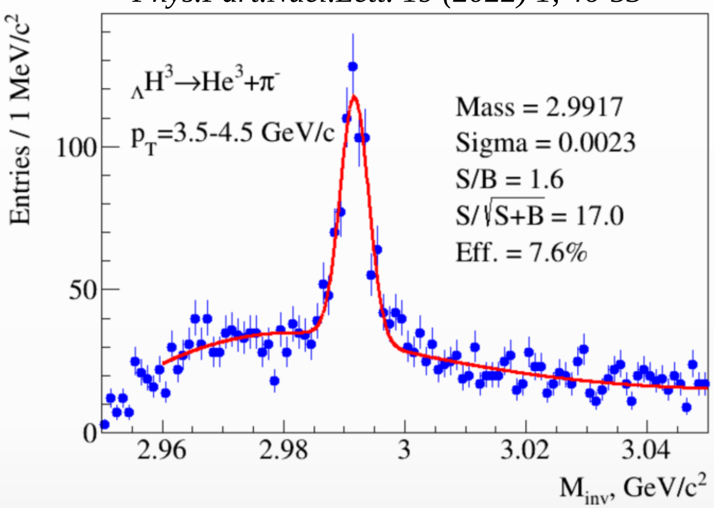

Phys. Lett. B697 (2011) 203

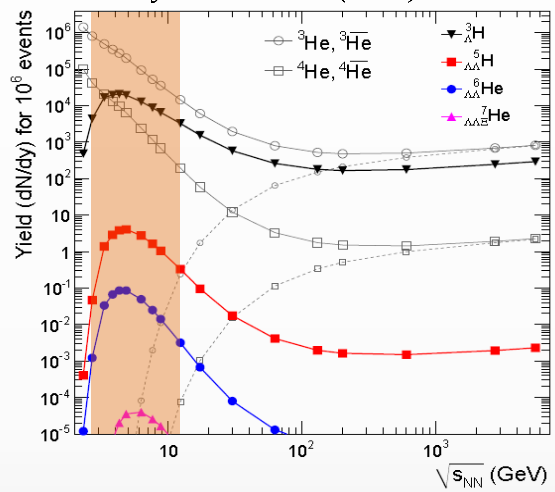

Thermal model predicts an enhanced hypernuclear production in the NICA energy range

Spectrum is reconstructed up to p_T=4.5 GeV/c

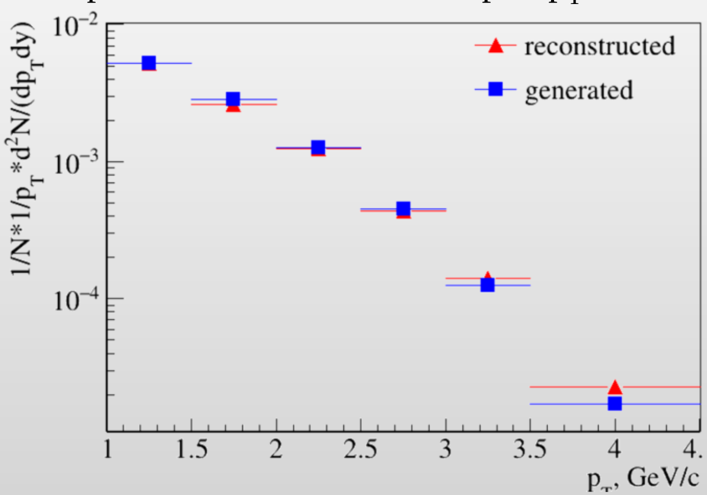

✓ dN/dt = p0*exp(-t/p1), p1 - lifetime

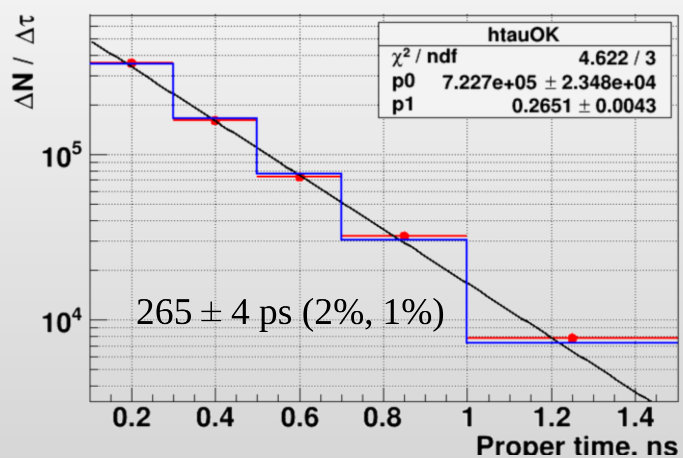

BM@N (Baryonic Matter at Nuclotron)

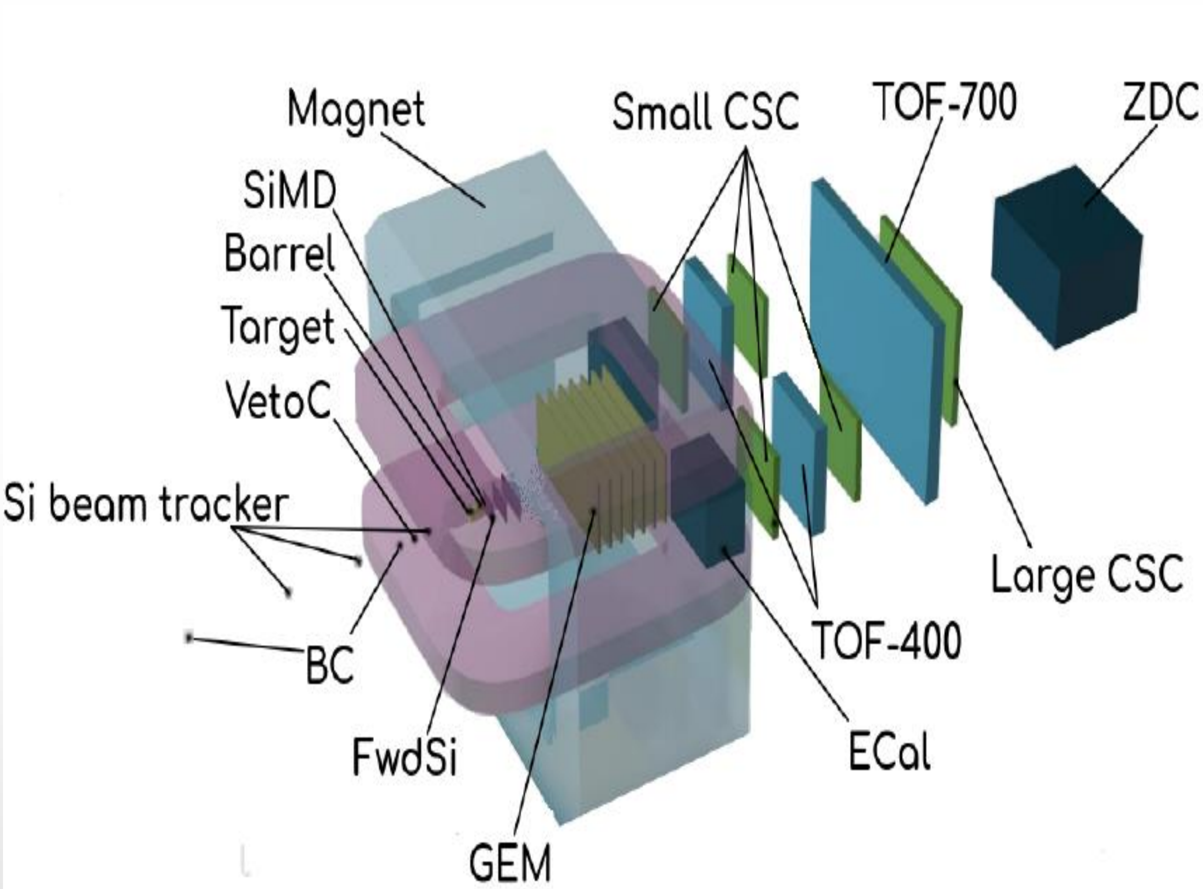

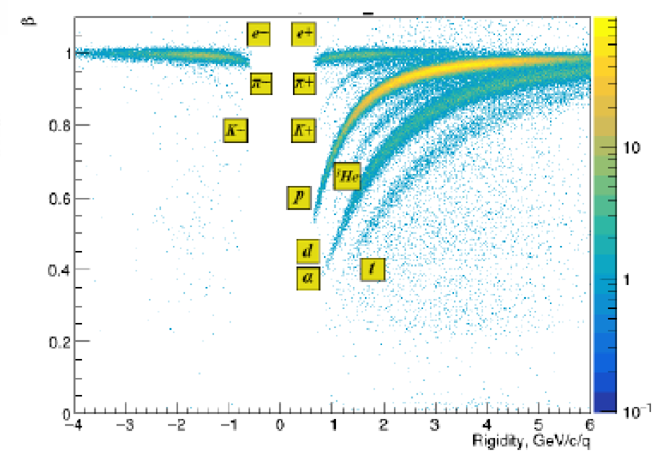

- Ar+A @ 3.2 AGeV
- Λ^0 mass resolution is about 3.3MeV/c^2

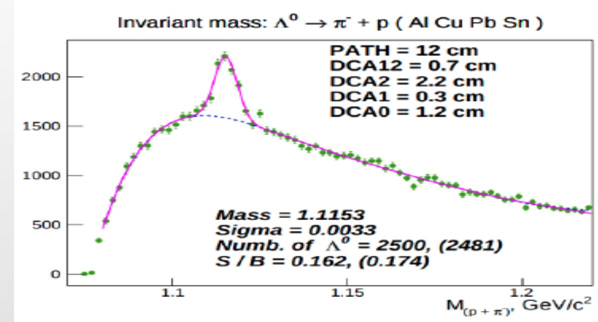

October 2022: first physics run with Xe+CsI ($\sqrt{s_{NN}}$ = 2.3-3.3 GeV) with beam intensity ~ 2*10^5 /s (DAQ rate 2*10^3 /s)

Relativistic Heavy-Ion Collisions and QCD Phase Diagram

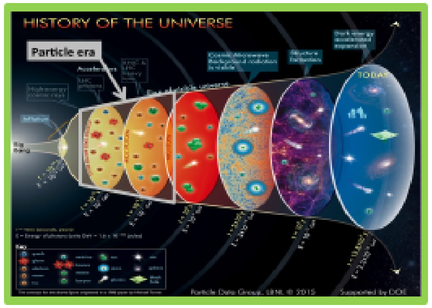

High temperature:
Early Universe evolution

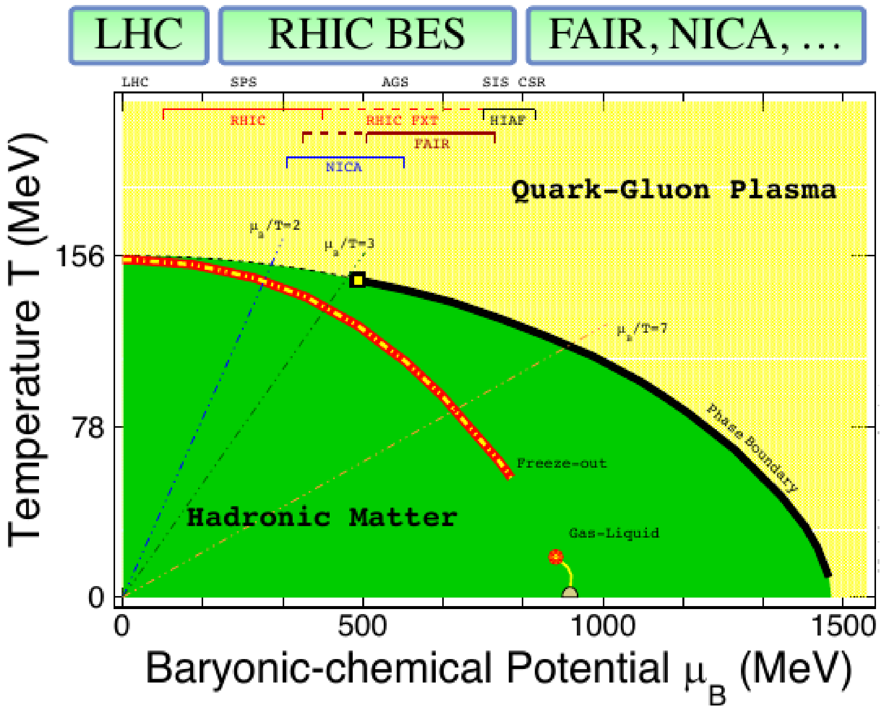

High baryon density:
Inner structure of
compact stars

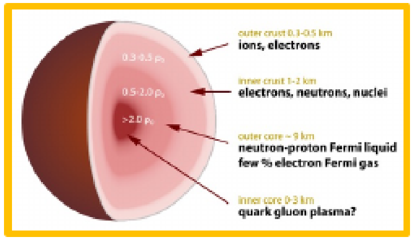

1) At $\mu_B = 0$, smooth crossover (LGT + data) ;

2) Large μ_B, 1st order phase transition → **QCD critical point**

HADRON **QGP**

Bevalac ~1 GeV → **AGS** ~5 GeV → **SPS** ~20 GeV → **RHIC** ~100 GeV → **LHC** ~5000 GeV

FAIR; NICA ← **RHIC/BES** ←

QGP may be produced at low energies; QGP is produced in high energy collisions

2022: 17 years of the "perfect fluid" found at RHIC

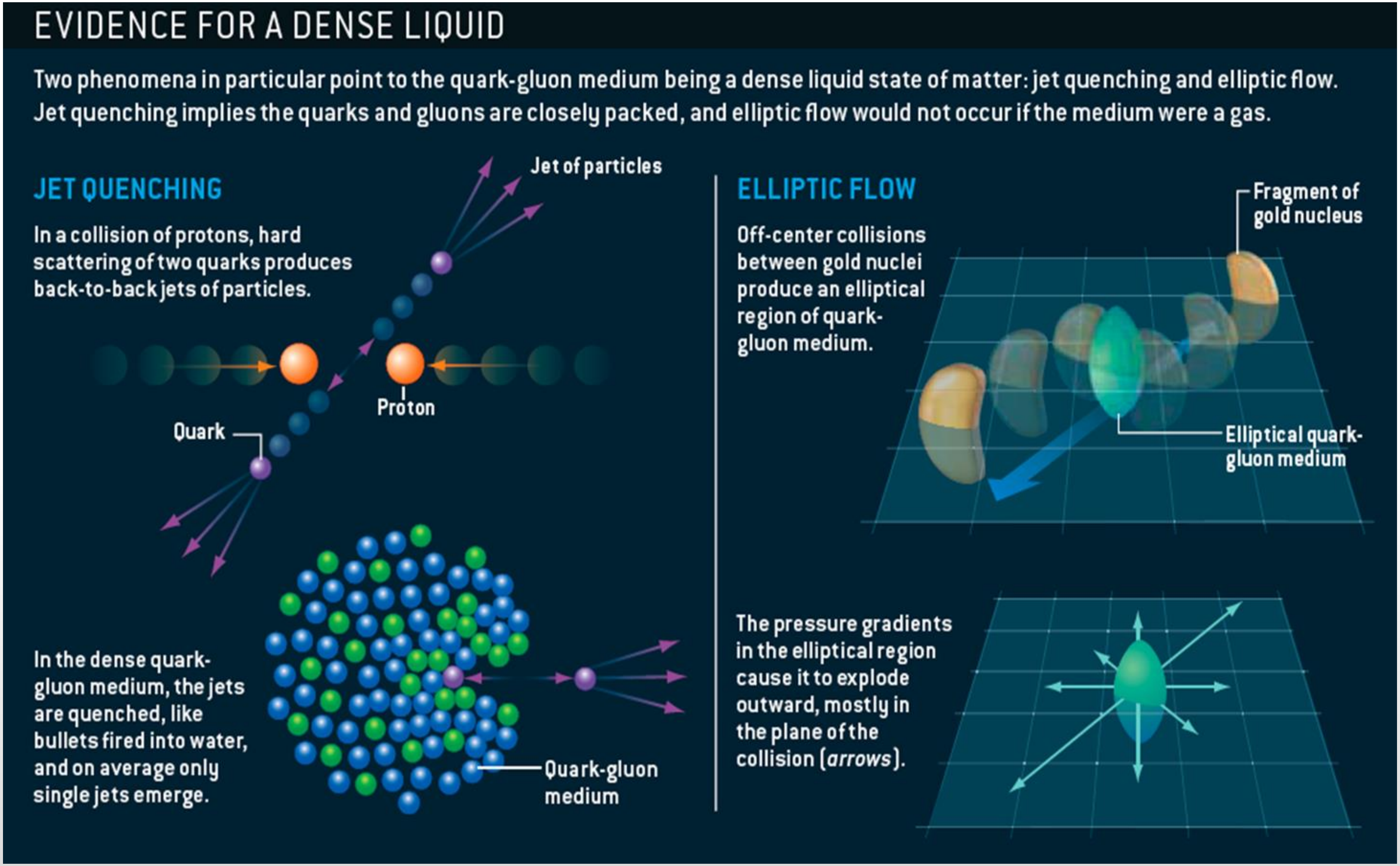

M. Roirdan and W. Zajc,
Scientific American, May 2006

Flow at AGS: Constraints for the Hadronic EOS

Danielewicz, Lacey, Lynch, Science 298 (2002) 1592-1596

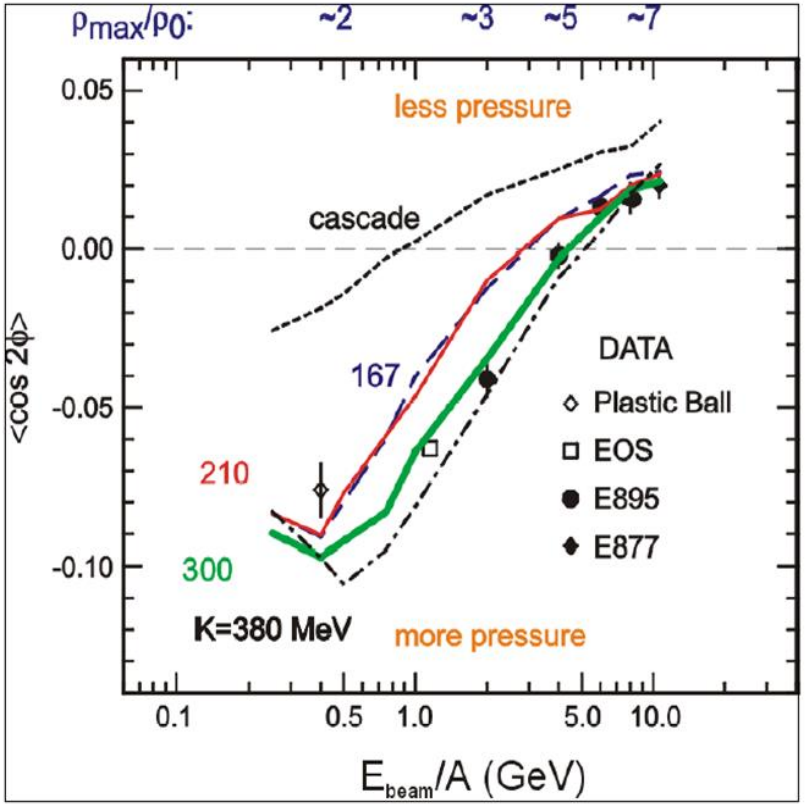

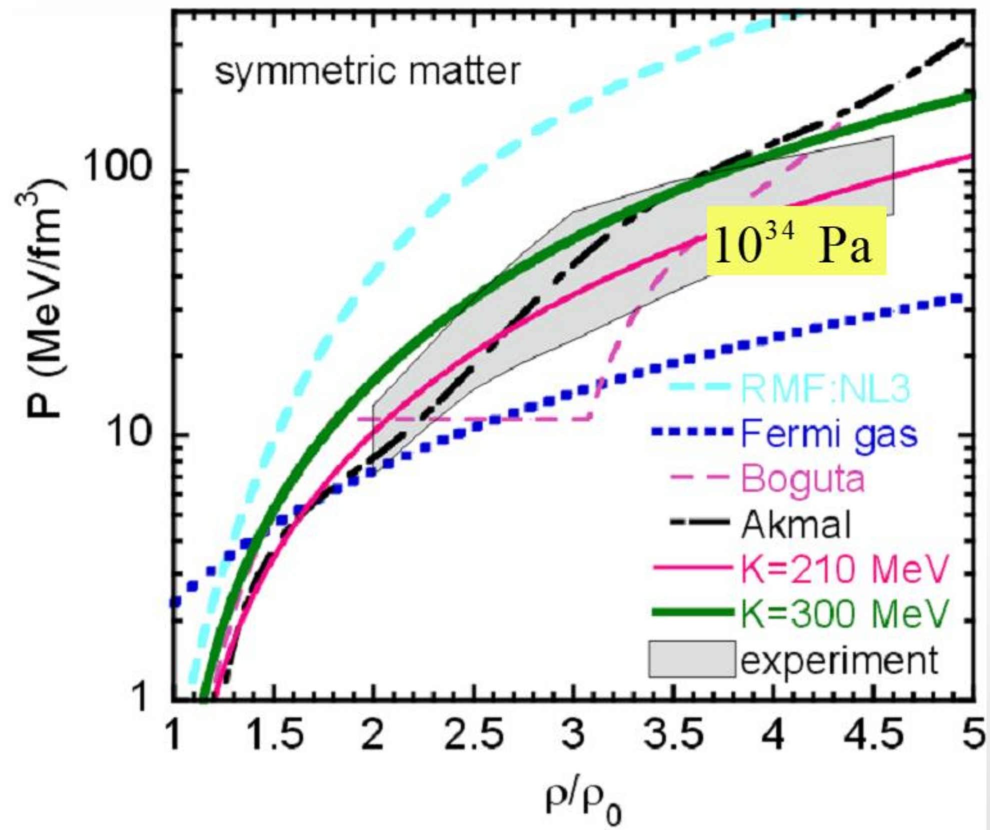

Passage time: **$2R/(\beta_{cm}\gamma_{cm})$**

Expansion time: **R/c_s**

$c_s = c\sqrt{dp/d\varepsilon}$ - speed of sound

$$c_s = \sqrt{K/9m_N} \approx 0.15c, 0.21c$$

Flow at AGS/Nuclotron = Interplay of passage/expansion times

Anisotropic Flow at RHIC-LHC

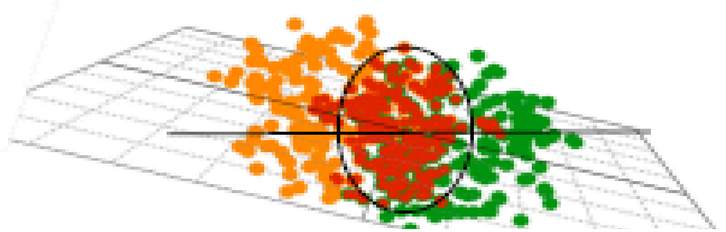

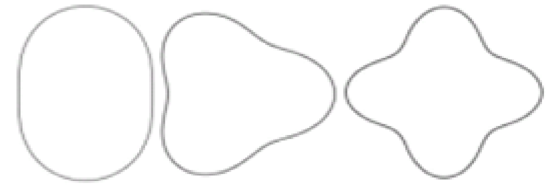

$$\epsilon_n = \sqrt{\frac{\langle r^n \cos n\phi\rangle + \langle r^n \sin n\phi\rangle}{\langle r^n\rangle}}$$

$$\frac{dN}{d\phi} \propto \left(1 + 2\sum_{n=1} v_n \cos\left[n\left(\phi - \Psi_n\right)\right]\right)$$

Initial eccentricity (and its attendant fluctuations) ε_n drive momentum anisotropy v_n with specific viscous modulation

Gale, Jeon, et al., Phys. Rev. Lett. 110, 012302

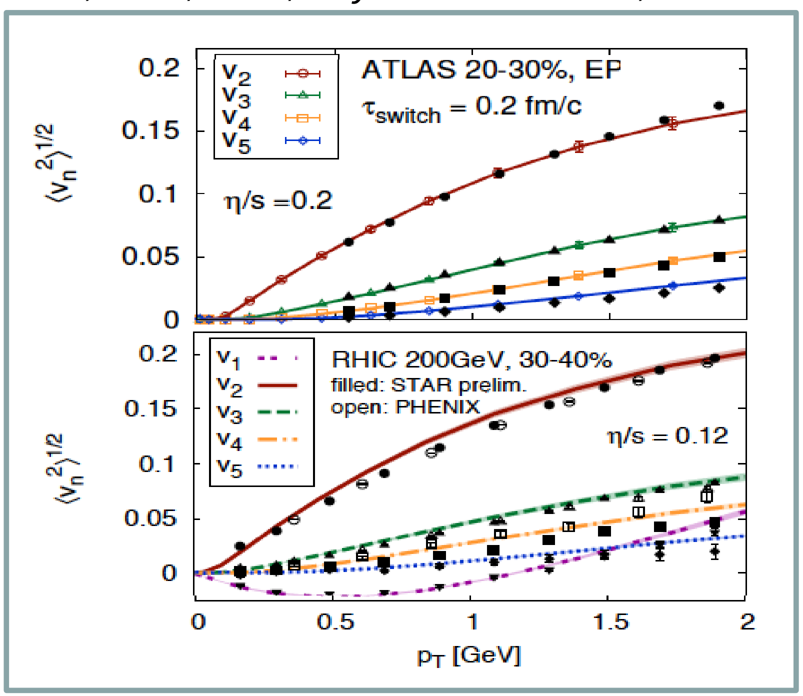

Phys. Rev. Lett. 122 (2019) 172301

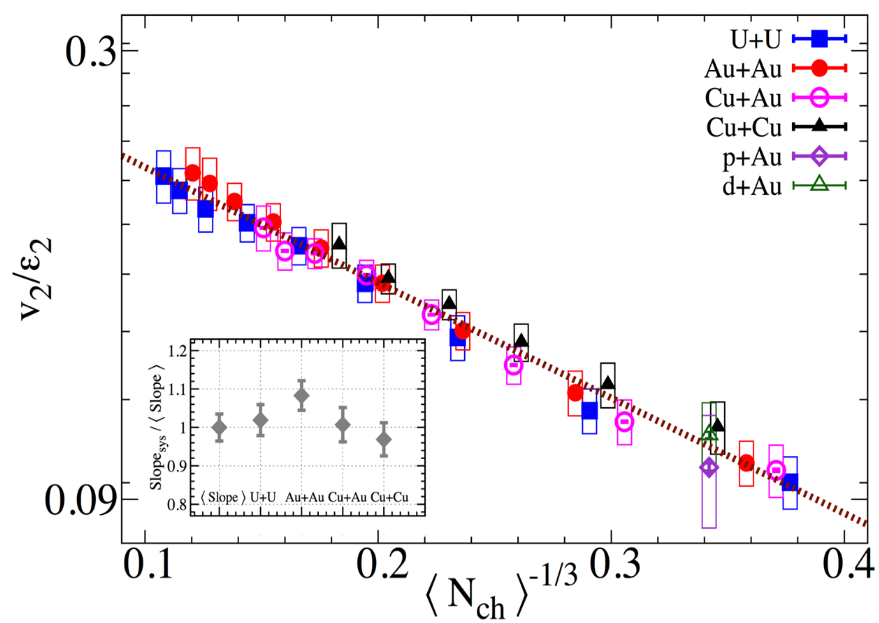

vHLLE+UrQMD: Elliptic and triangular flow in Au + Au collisions at 200 GeV

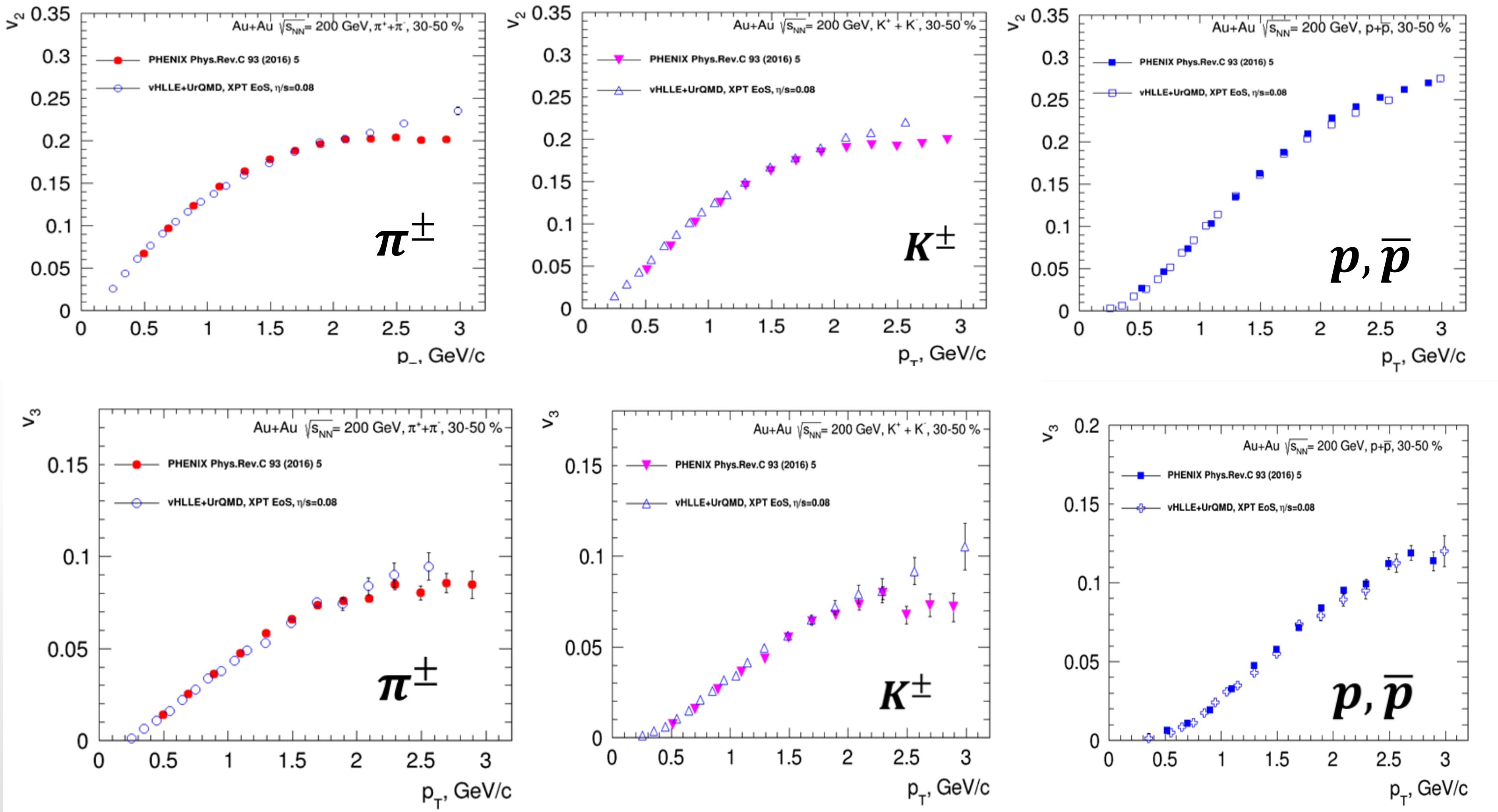

3D hydro model vHHLE + UrQMD (XPT EOS), $\eta/s = 0.08$

Reasonable agreement between results of vHLLE+UrQMD model and published PHENIX data

GLOBAL BAYESIAN CONSTRAINTS ON QGP VISCOSITY

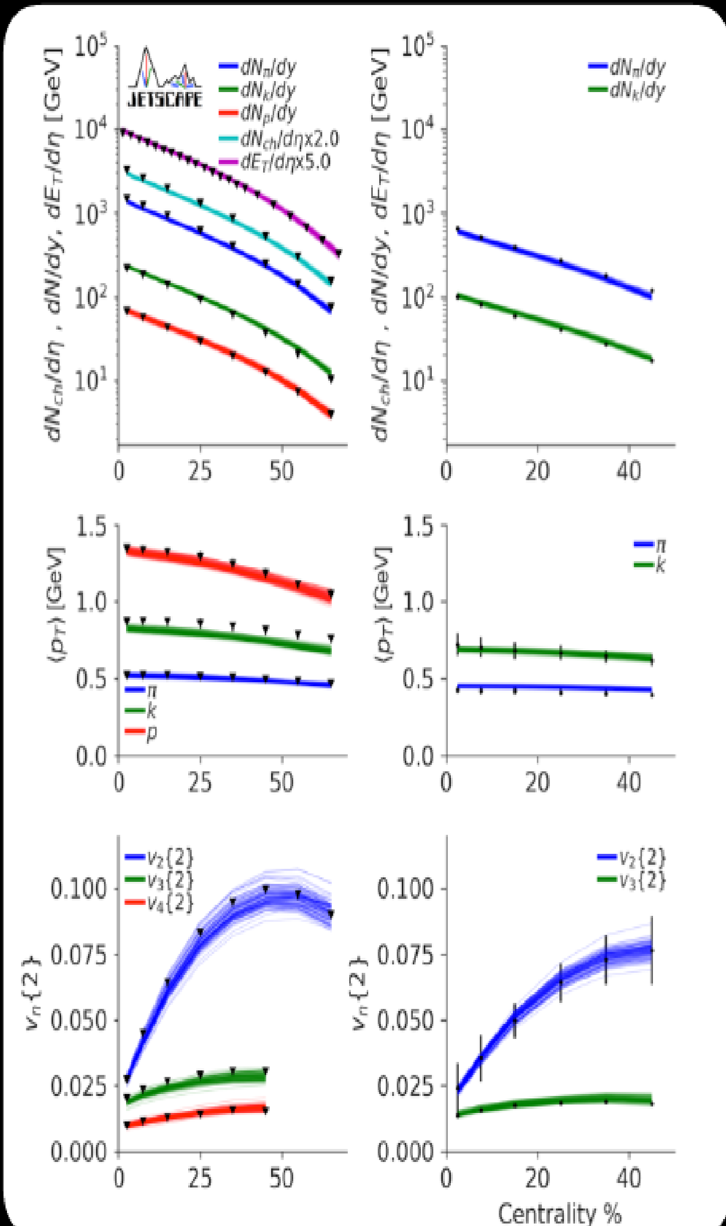

S. Pratt, E. Sangaline, P. Sorensen and H. Wang, Phys. Rev. Lett. 114, 202301 (2015)

J. E. Bernhard, J. S. Moreland, S. A. Bass, J. Liu and U. Heinz, Phys. Rev. C94, 024907 (2016)

J. E. Bernhard, J. S. Moreland and S. A. Bass, Nature Phys. 15, 1113-1117 (2019)

G. Nijs, W. Van Der Schee, U. Gursoy and R. Snellings,
Phys. Rev. Lett. 126, 202301 (2021) & Phys. Rev. C103, 054909 (2021)

D. Everett *et al.* [JETSCAPE], Phys. Rev. Lett. 126, 242301 & Phys. Rev. C103, 054904 (2021)

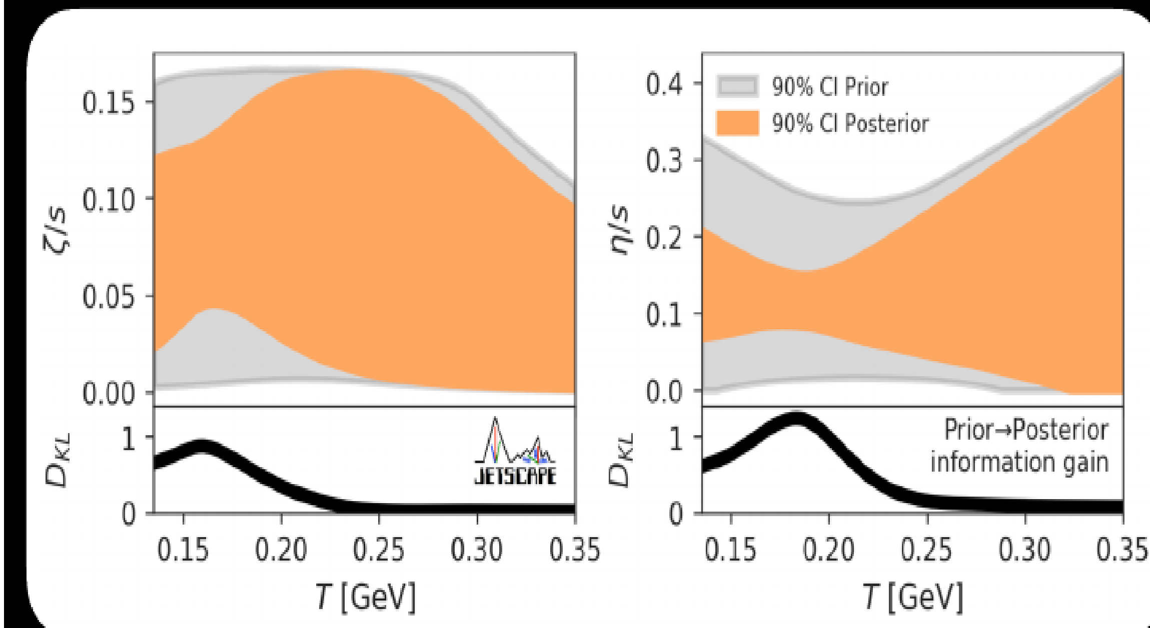

- Precision hadronic measurements can systematically constrain the QGP viscosity

Collision Energy and System Scan Programs

HADES BES (SIS): Au+Au at $\sqrt{s_{NN}}$ = 2.42 GeV, Ag+Ag at $\sqrt{s_{NN}}$ = 2.42 GeV, 2.55 GeV.

STAR BES (RHIC): Au+Au at $\sqrt{s_{NN}}$ = 3-200 GeV

NA61/SHINE (SPS): Be+Be, Ar+Sc, Xe+La, Pb+Pb at $\sqrt{s_{NN}}$ = 5.1-17.3 GeV

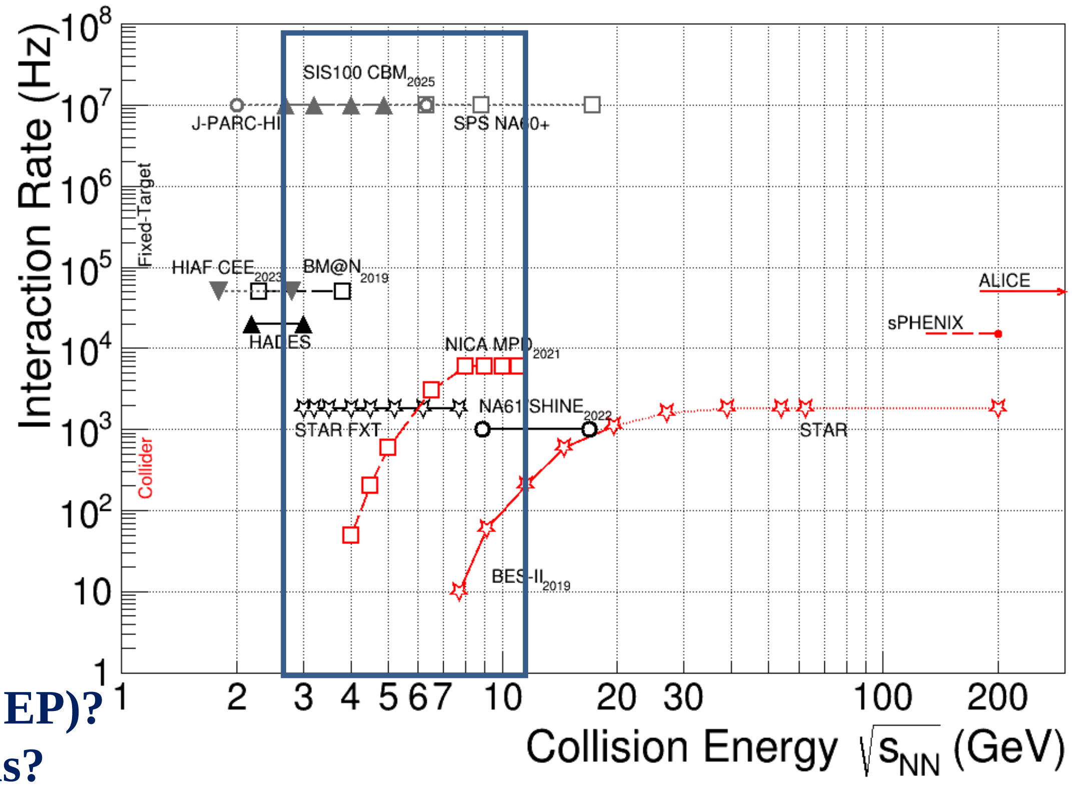

- **Map turn-off of QGP signatures**
- **Location of the Critical End Point (CEP)?**
- **Location of phase coexistence regions?**
- **1st order phase transition signs**
- **Detailed properties of each phase?**

$$\frac{\eta}{s}(T,\mu),\ \frac{\zeta}{s}(T,\mu),\ c_s(T),\ \hat{q}(T),\ \alpha_s(T),\ \text{etc}$$

STAR BES-I and BES-II Data Sets

Au+Au Collisions at RHIC

Collider Runs						Fixed-Target Runs					
	$\sqrt{s_{NN}}$ (GeV)	#Events	μ_B	y_{beam}	run		$\sqrt{s_{NN}}$ (GeV)	#Events	μ_B	y_{beam}	run
1	200	380 M	25 MeV	5.3	Run-10, 19	1	13.7 (100)	50 M	280 MeV	-2.69	Run-21
2	62.4	46 M	75 MeV		Run-10	2	11.5 (70)	50 M	320 MeV	-2.51	Run-21
3	54.4	1200 M	85 MeV		Run-17	3	9.2 (44.5)	50 M	370 MeV	-2.28	Run-21
4	39	86 M	112 MeV		Run-10	4	7.7 (31.2)	260 M	420 MeV	-2.1	Run-18, 19, 20
5	27	585 M	156 MeV	3.36	Run-11, 18	5	7.2 (26.5)	470 M	440 MeV	-2.02	Run-18, 20
6	19.6	595 M	206 MeV	3.1	Run-11, 19	6	6.2 (19.5)	120 M	490 MeV	1.87	Run-20
7	17.3	256 M	230 MeV		Run-21	7	5.2 (13.5)	100 M	540 MeV	-1.68	Run-20
8	14.6	340 M	262 MeV		Run-14, 19	8	4.5 (9.8)	110 M	590 MeV	-1.52	Run-20
9	11.5	157 M	316 MeV		Run-10, 20	9	3.9 (7.3)	120 M	633 MeV	-1.37	Run-20
10	9.2	160 M	372 MeV		Run-10, 20	10	3.5 (5.75)	120 M	670 MeV	-1.2	Run-20
11	7.7	104 M	420 MeV		Run-21	11	3.2 (4.59)	200 M	699 MeV	-1.13	Run-19
						12	3.0 (3.85)	2000 M	750 MeV	-1.05	Run-18, 21

Precision data to map the QCD phase diagram

$3 < \sqrt{s_{NN}} < 200$ GeV; $750 < \mu_B < 25$ MeV

Beam Energy Dependence of Directed Flow (v_1)

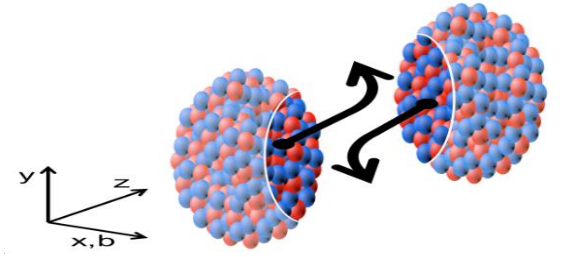

- ***Generated during the nuclear passage time (2R/γ) – sensitive to EOS***
- ***RHIC 200 GeV (2R/γ) ~ 0.1 fm/c***
- ***AGS: 3-4.5 GeV (2R/γ) ~ 9-5 fm/c***

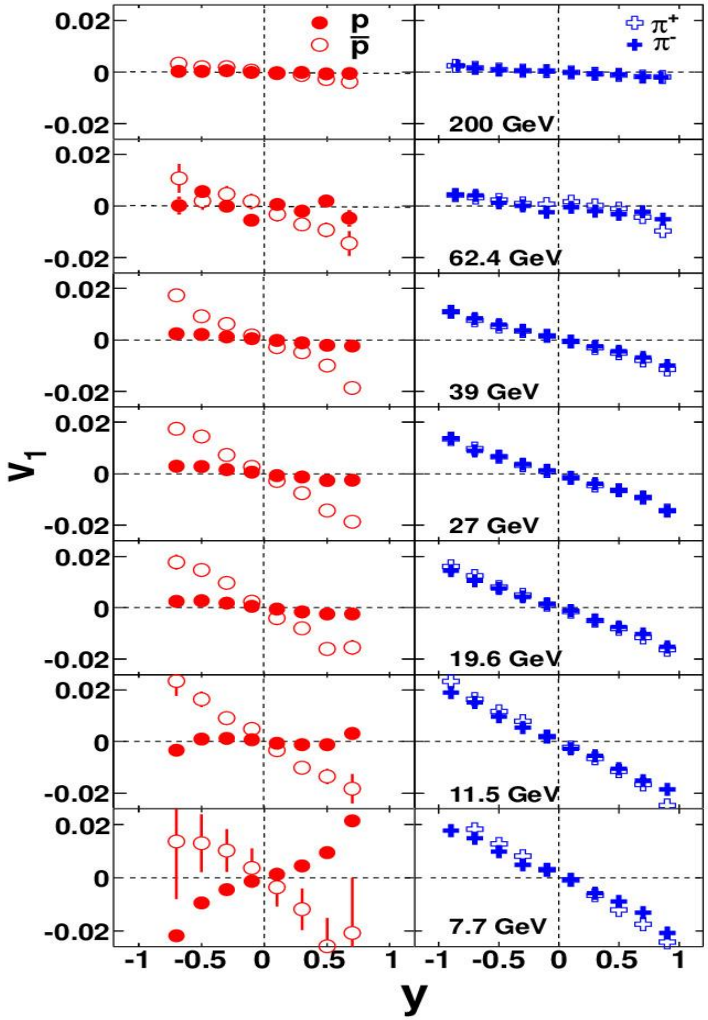

STAR: Phys.Rev.Lett. 112 (2014)

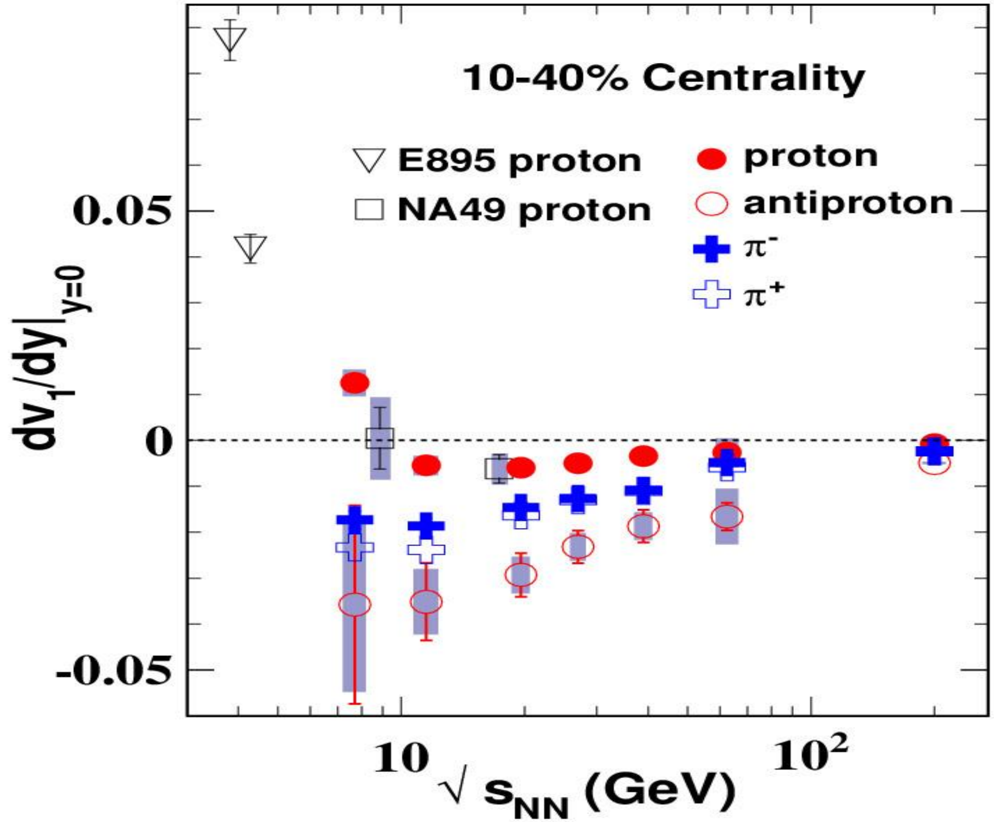

Trend observed by STAR inline with NA49 and E895 data

Beam Energy Dependence of Directed Flow (v_1)

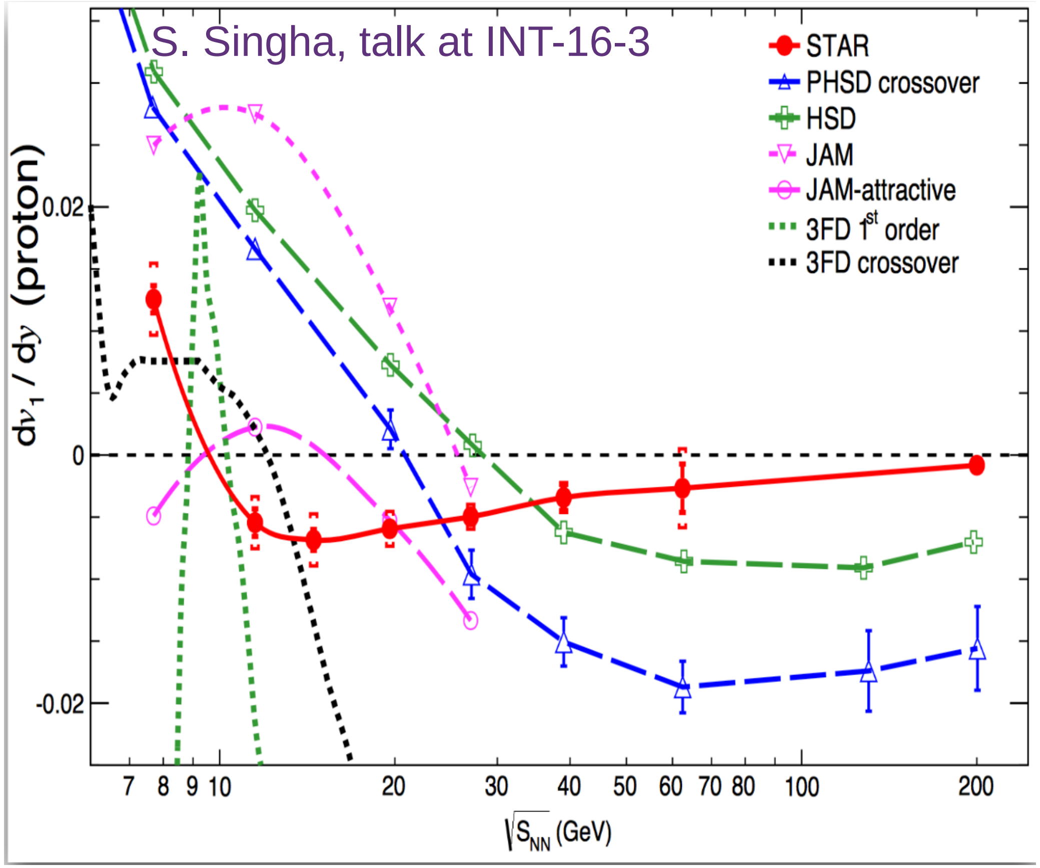

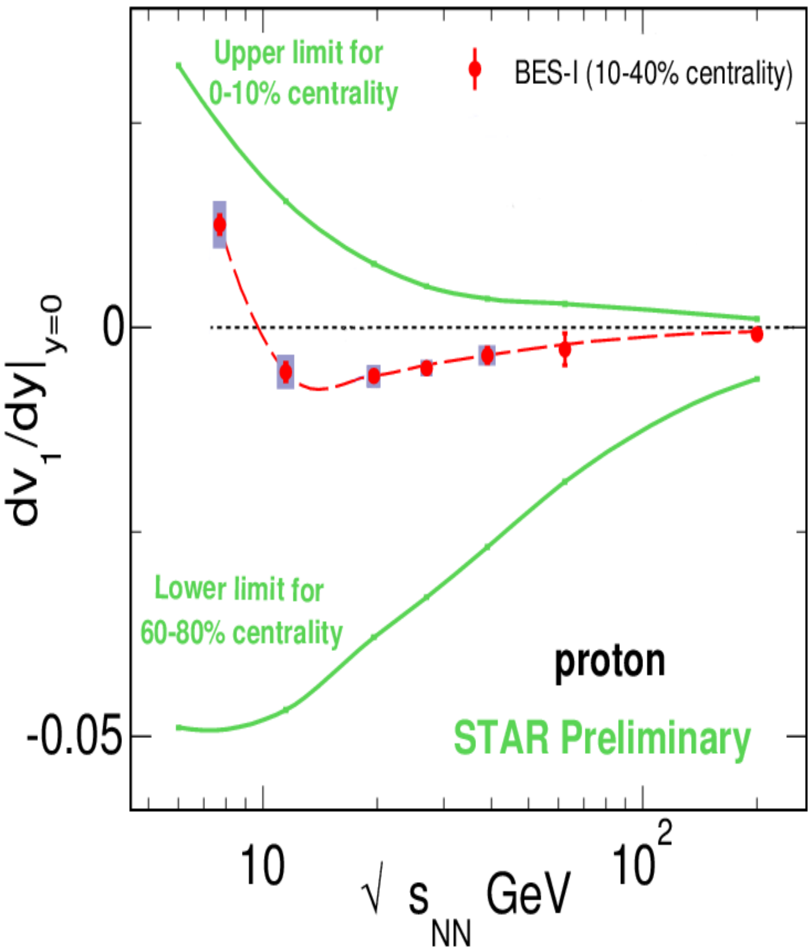

None of the models explains the data

- ***Systematics associated with the models is quite large***

Global hyperon polarization at BES

- Lambdas are "self-analyzing"
  - Reveal polarization by preferentially emitting daughter proton in spin direction

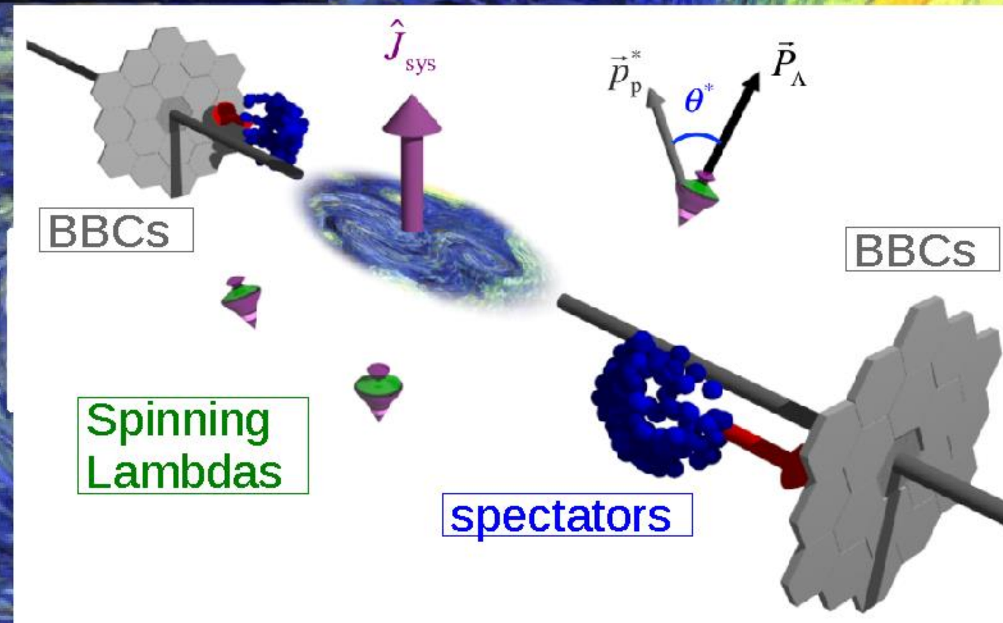

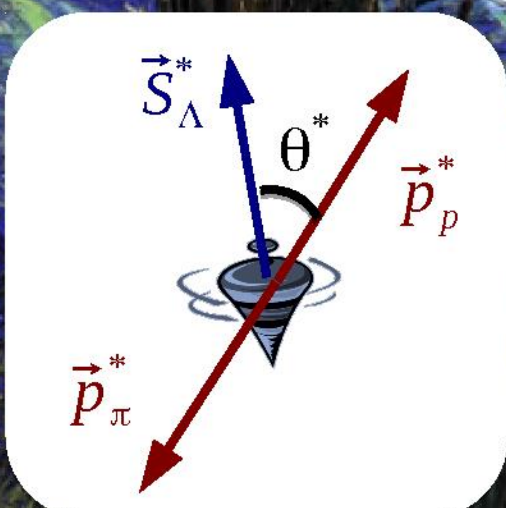

The global polarization observable is defined by [34]:

$$P_{\Lambda} = \frac{8}{\pi \alpha_{\Lambda}} \frac{\langle \sin(\Psi_{EP} - \phi^*_{p}) \rangle}{R_{EP}}. \quad (1)$$

Here $\alpha_{\Lambda} = 0.732 \pm 0.014$ [35] is the Λ decay parameter, Ψ_{EP} the event plane angle, ϕ^*_{p} the azimuthal angle of the proton in the Λ rest frame, R_{EP} the resolution of the event plane angle and the brackets $\langle . \rangle$ denote the average

Energy excitation function of global hyperon polarization

STAR Collaboration, Phys. Lett. B 827 (2022) 137003

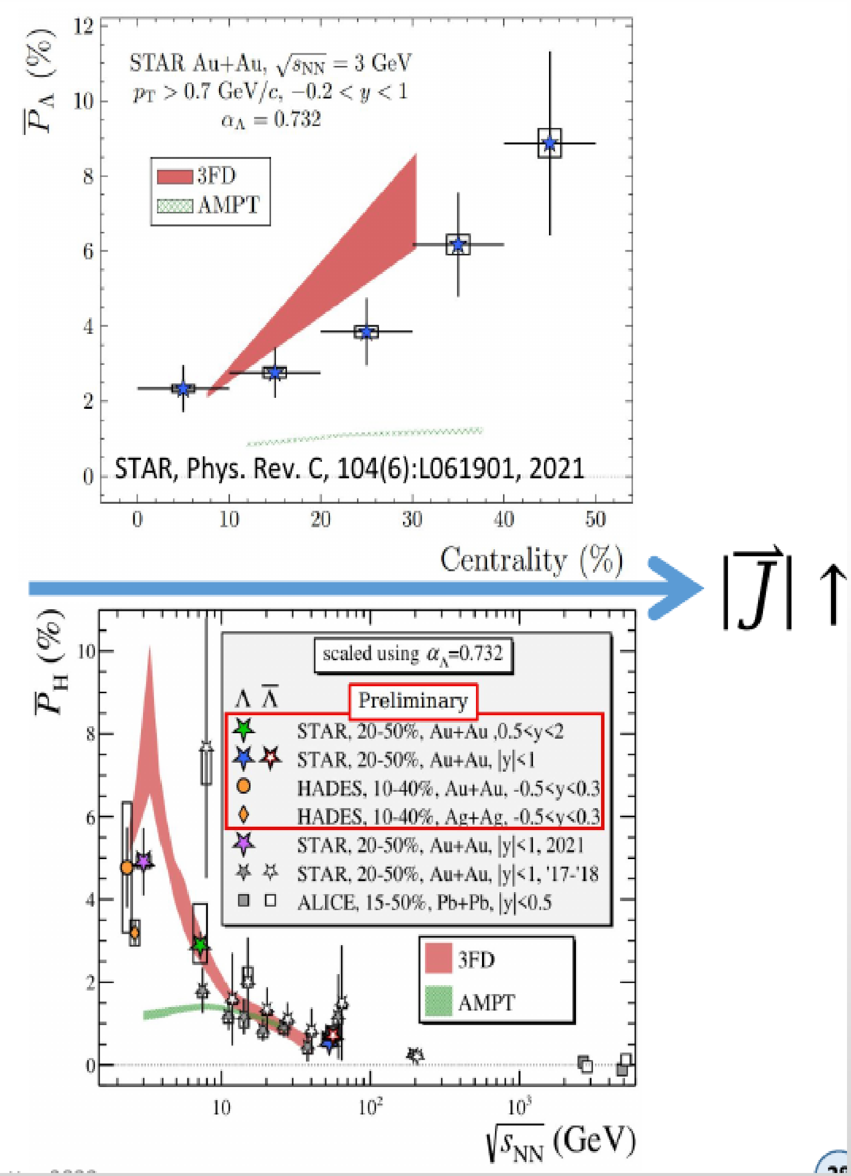

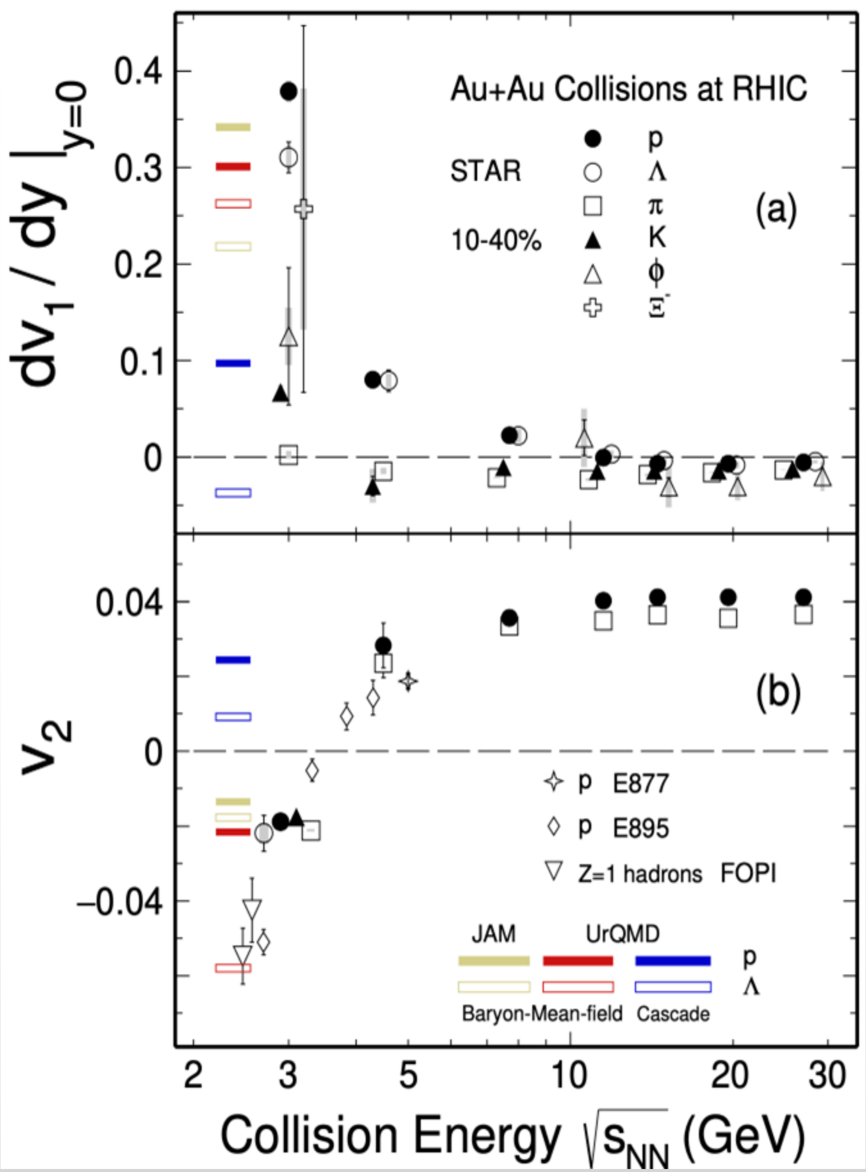

Energy excitation function of global hyperon polarization

Collision-energy dependence

- Theory and experiment have assumed alignment between system $\widehat{J}$ and mid-rapidity $\widehat{J}$
  - Experiment approximates $\widehat{J}_{\mathrm{syst}}$ with $\widehat{J}_{\mathrm{spec}}$
  - This *would* be a good approximation if spectator and mid-rapidity regions touch
- With a gap, these angular momenta are decorrelated

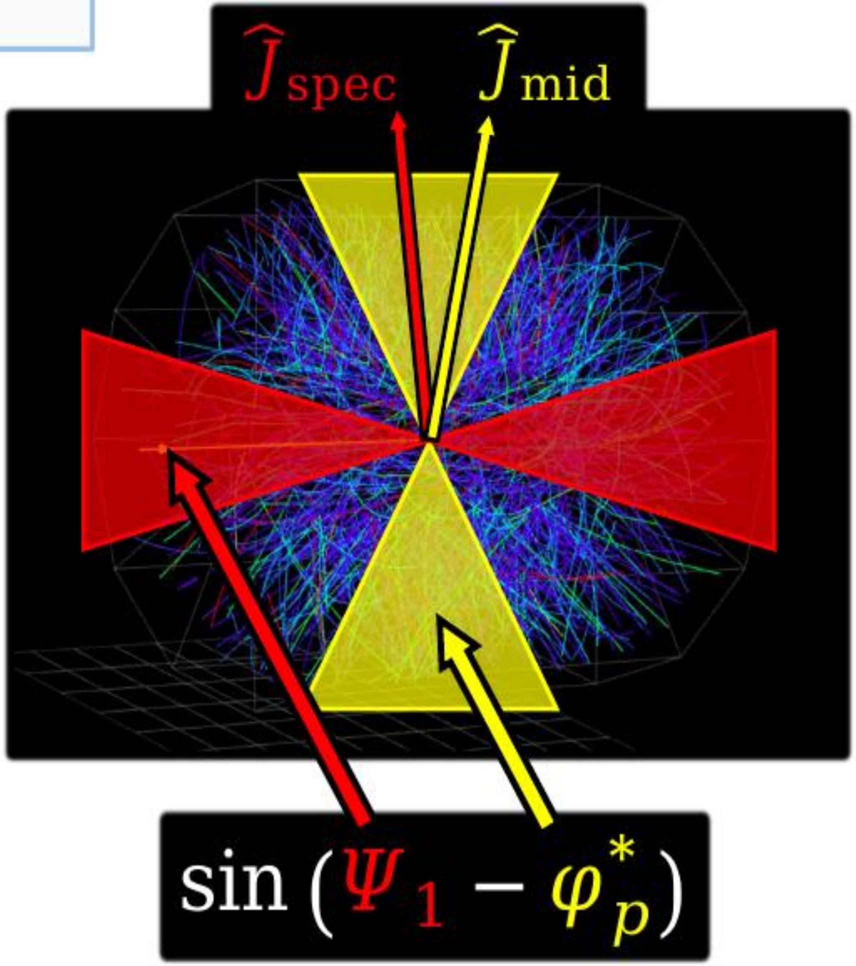

Correlation of interest

Beam Energy Dependence of Elliptic Flow (v_2)

EPJ Web Conf. 204 (2019) 03009

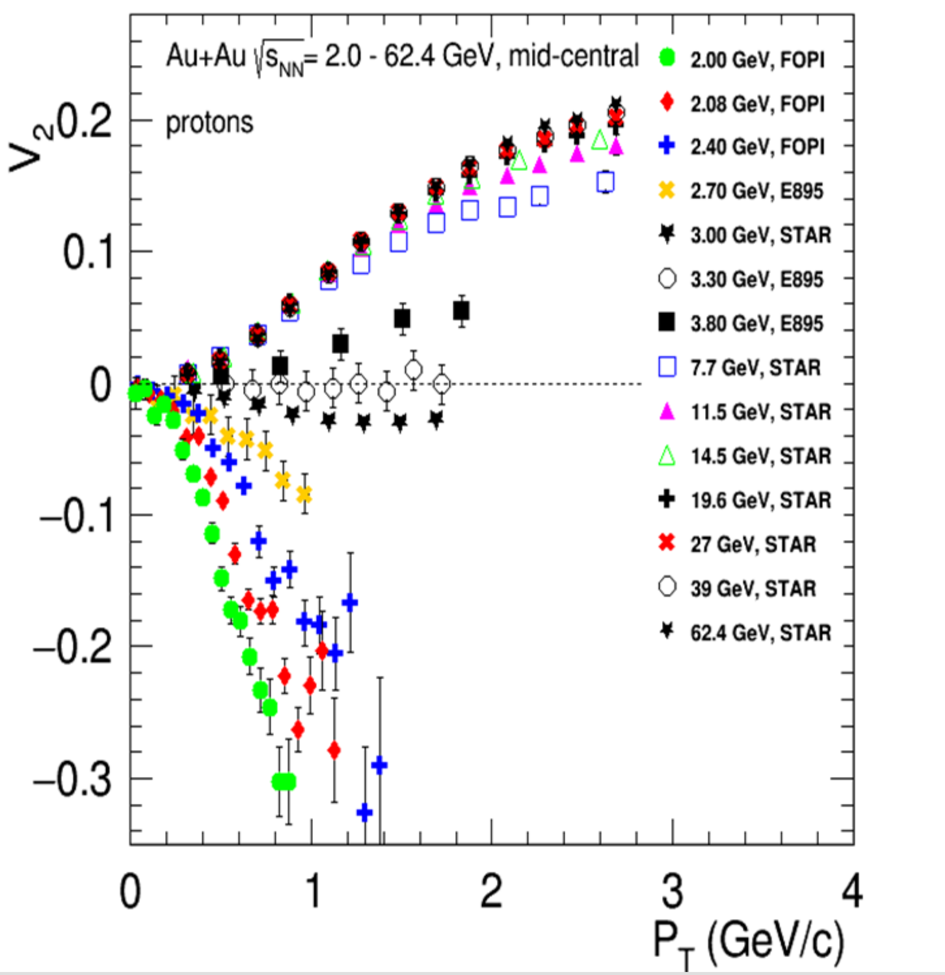

Phys. Rev. C 97, 064913 (2018)

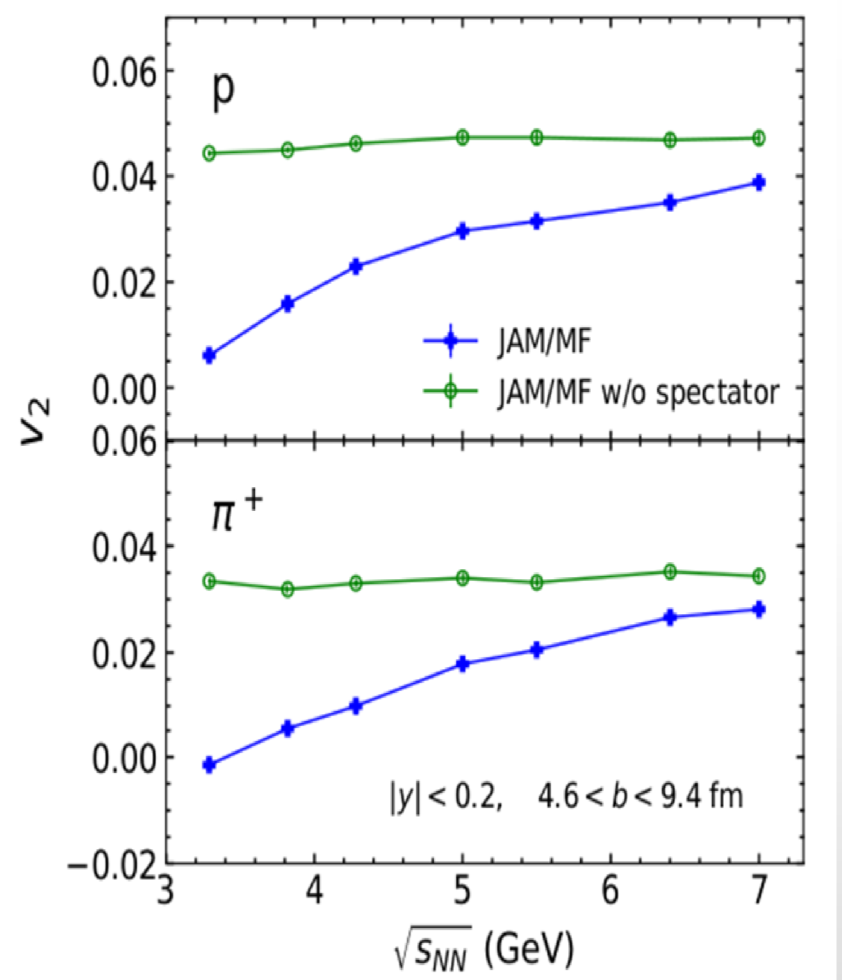

- **Strong energy dependence of v_2 at $\sqrt{s_{NN}}$ = 3-11 GeV**
  - $v_2 \approx 0$ at $\sqrt{s_{NN}}$ = 3.3 GeV and negative below

Elliptic Flow (v_2) at NICA energies: Models vs Data

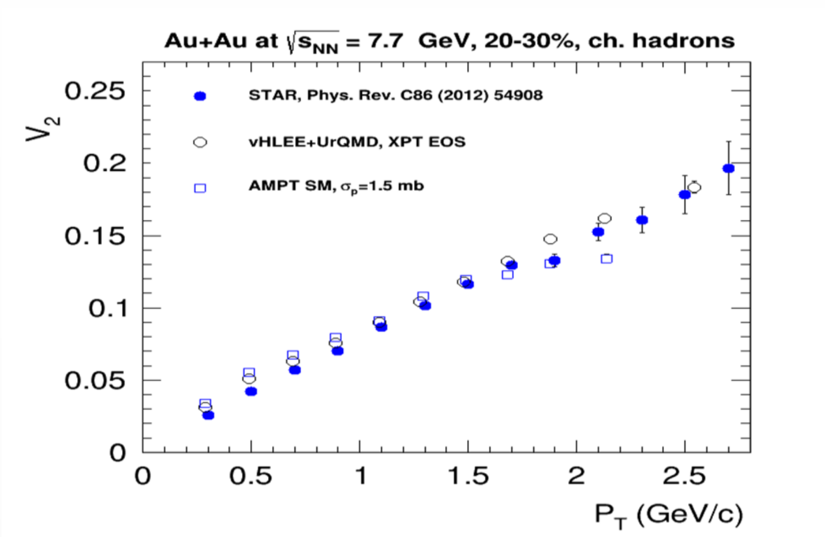

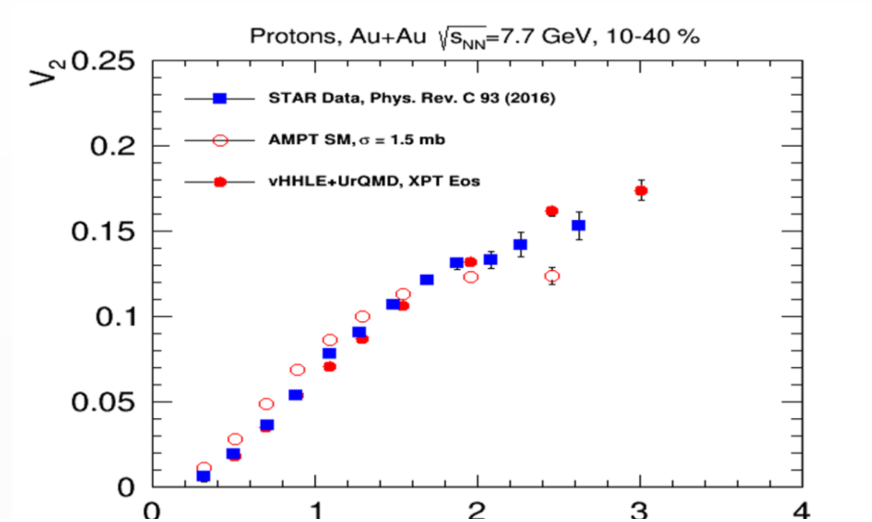

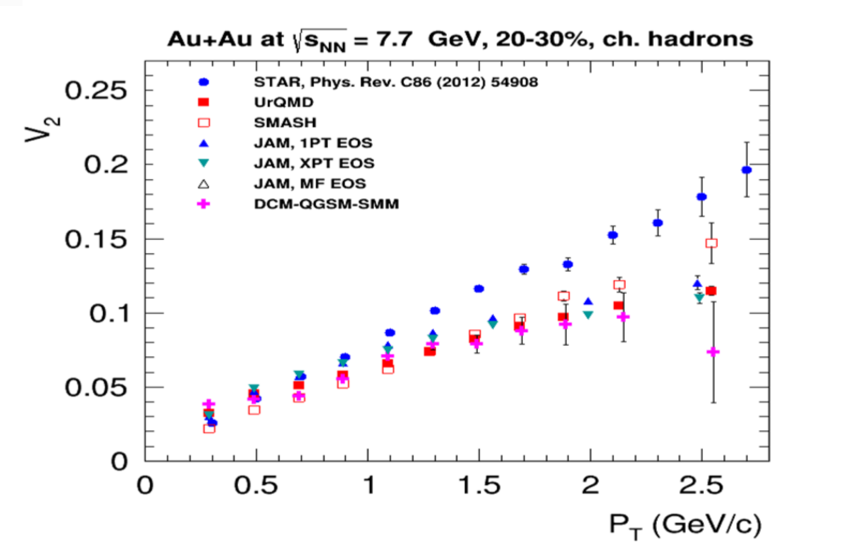

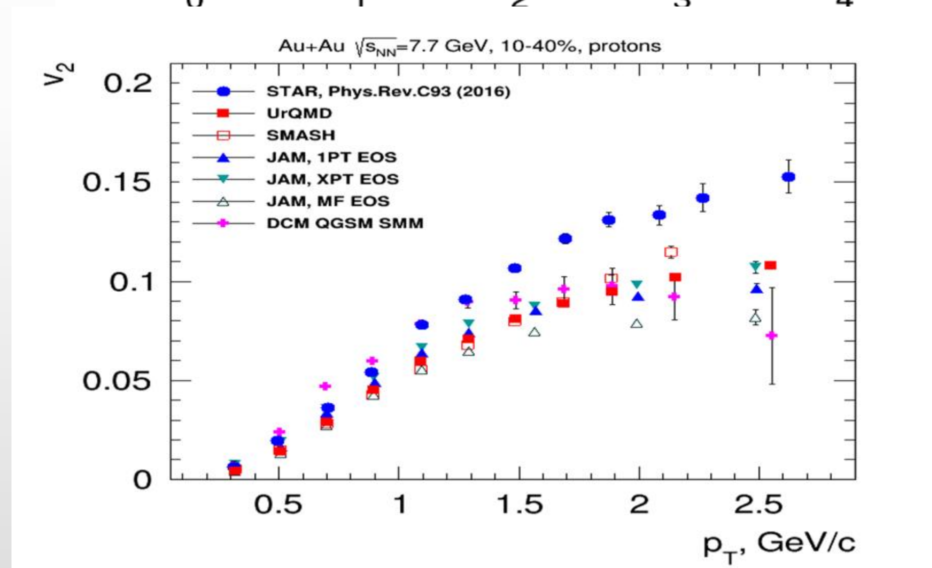

at $\sqrt{s_{NN}} \geq 7.7$ GeV pure string/hadronic cascade models underestimate v_2 – need hybrid models with QGP phase (vHLLE+UrQMD, AMPT with string melting,…)

Anisotropic Flow at Nuclotron/NICA energies: Models vs Data

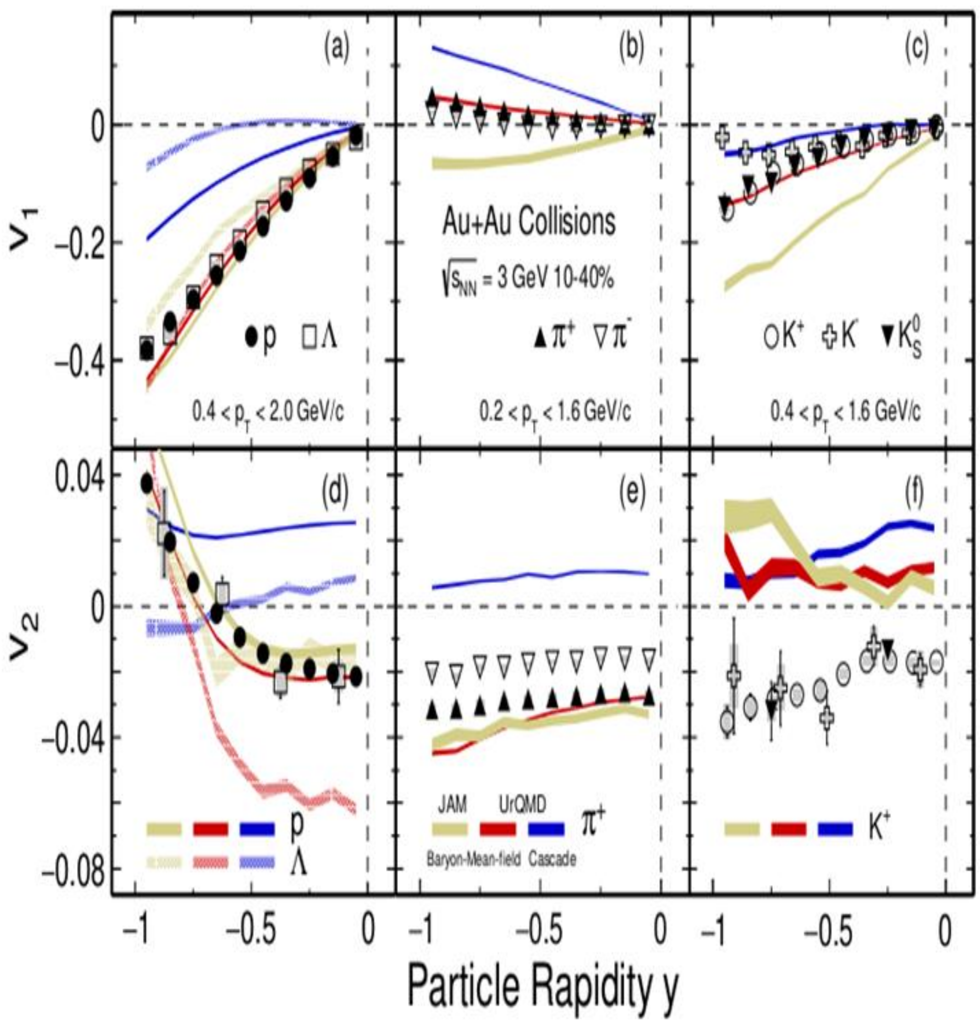

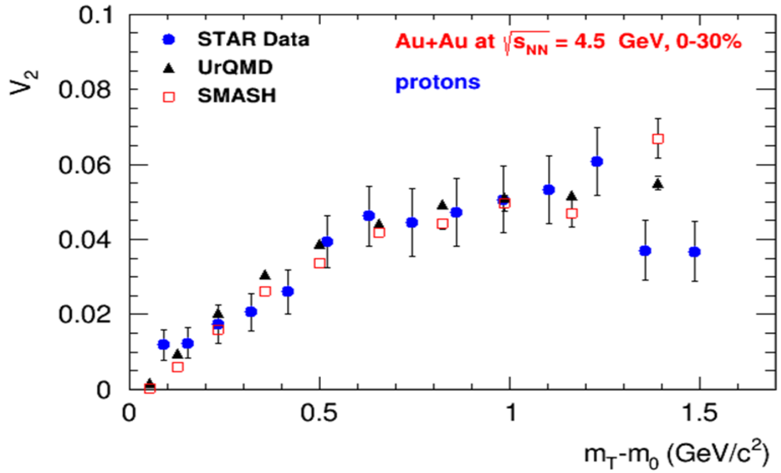

Phys.Rev.C 103 (2021) 3, 034908

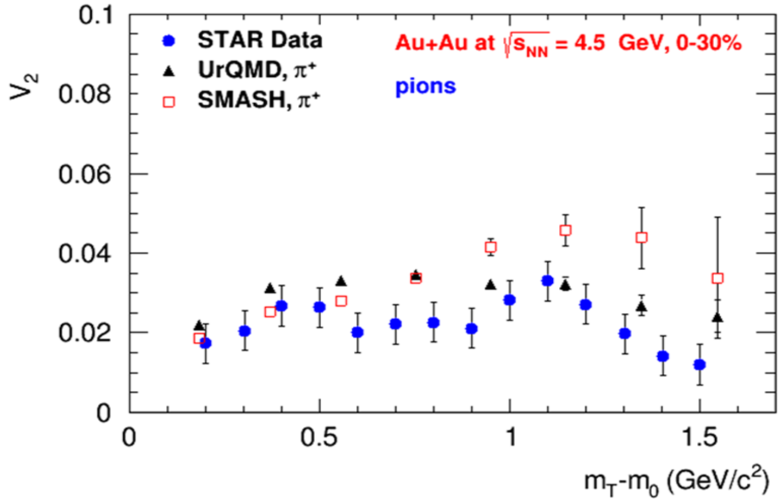

at $\sqrt{s_{NN}}$ ≥ 3-4.5 GeV pure hadronic models give similar v_2 signal compared to STAR data

Why do we need new measurements at BM@N and MPD?

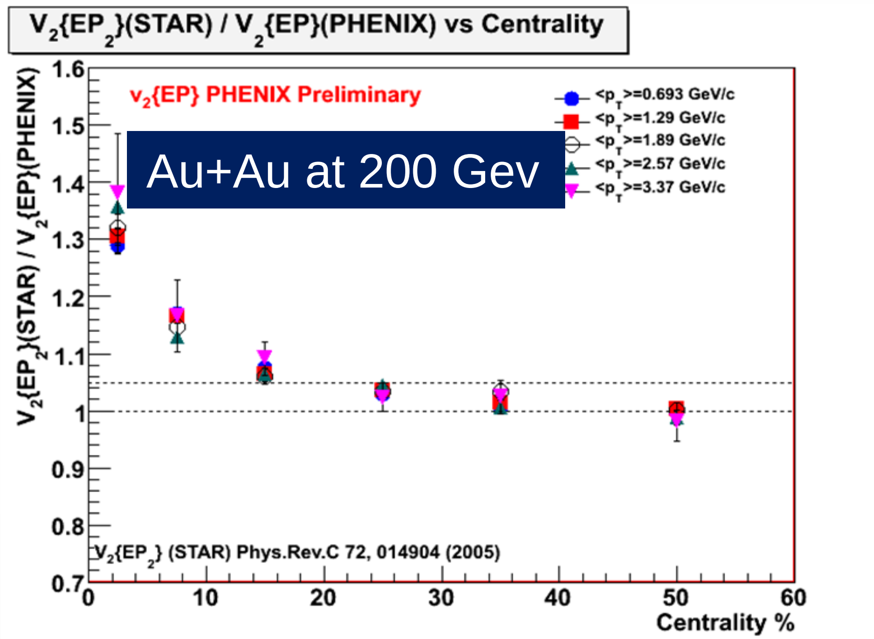

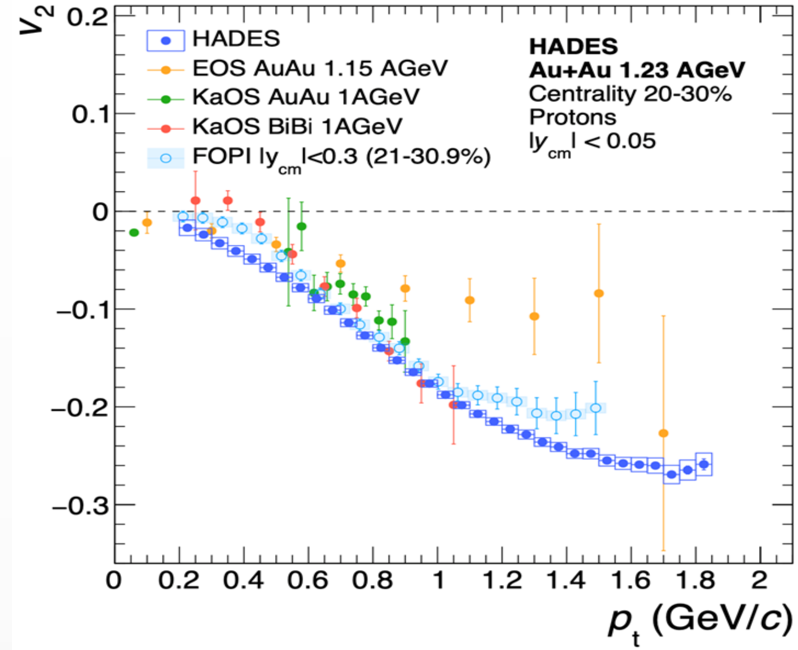

The main source of existing systematic errors in v_n measurements is the difference between results from different experiments at the same collision energy.

A good measurement should be reproducible; in particular, it should be done in such a way that one can easily compare results from different experiments, using different detectors.

For the sake of comparison with theory, an ideal measurement is a well-defined quantity that corresponds to a generic property of the system, closely related to an interesting theoretical concept.

"Eliminating experimental bias in anisotropic-flow measurements of high-energy nuclear collisions", Phys.Rev. C87 (2013) 4, 044907

Matthew Luzum, Jean-Yves Ollitrault

v_2 for pions and protons (MPD)

- Flow has high sensitivity to the transport properties of the QCD matter: EoS, speed of sound (c_s), specific viscosity (η/s), etc.
- Lack of existing differential measurements of v_n vs. p_T, centrality, species, etc.)
- 15 M of reconstructed UrQMD events for AuAu@7.7 GeV

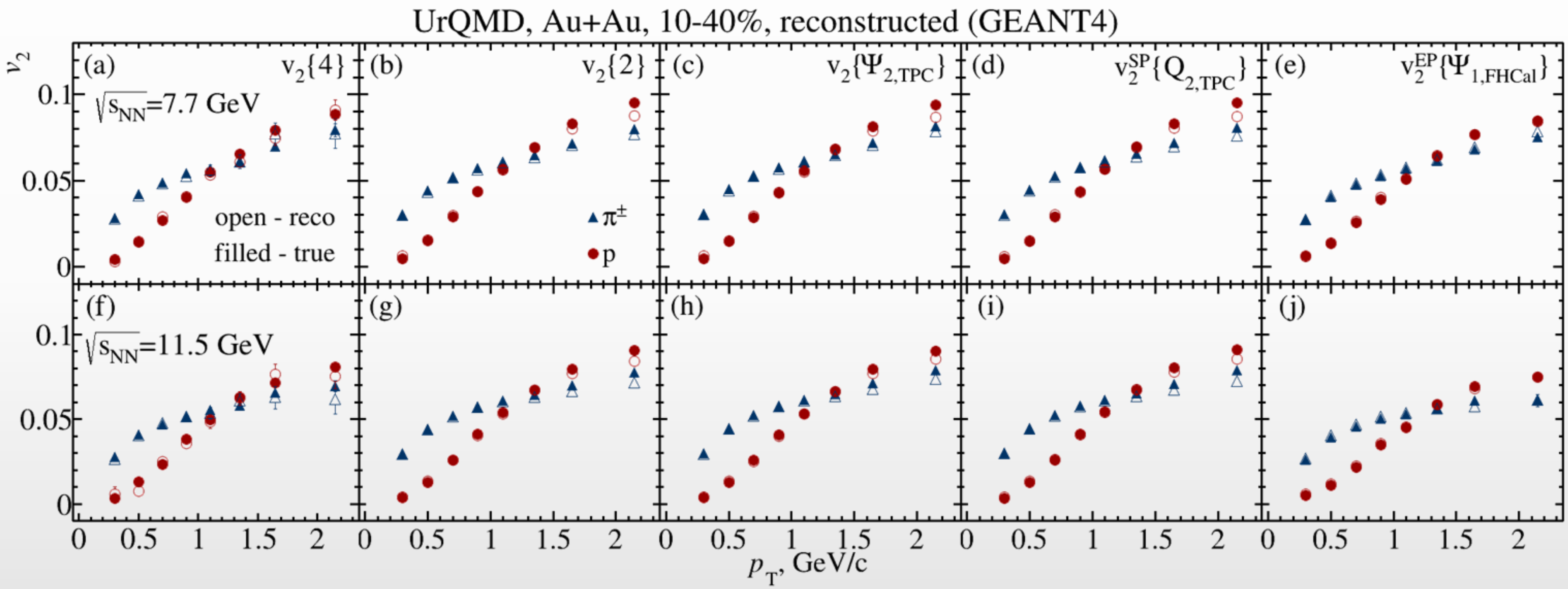

- Reconstructed and generated v_2 of pions and protons are in good agreement for all methods

Energy excitation function of k4/k2 in central Au+Au collisions

HADES: Phys.Rev.C 102 (2020) 2, 024914
STAR: Phys.Rev.Lett. 126 (2021) 9, 092301

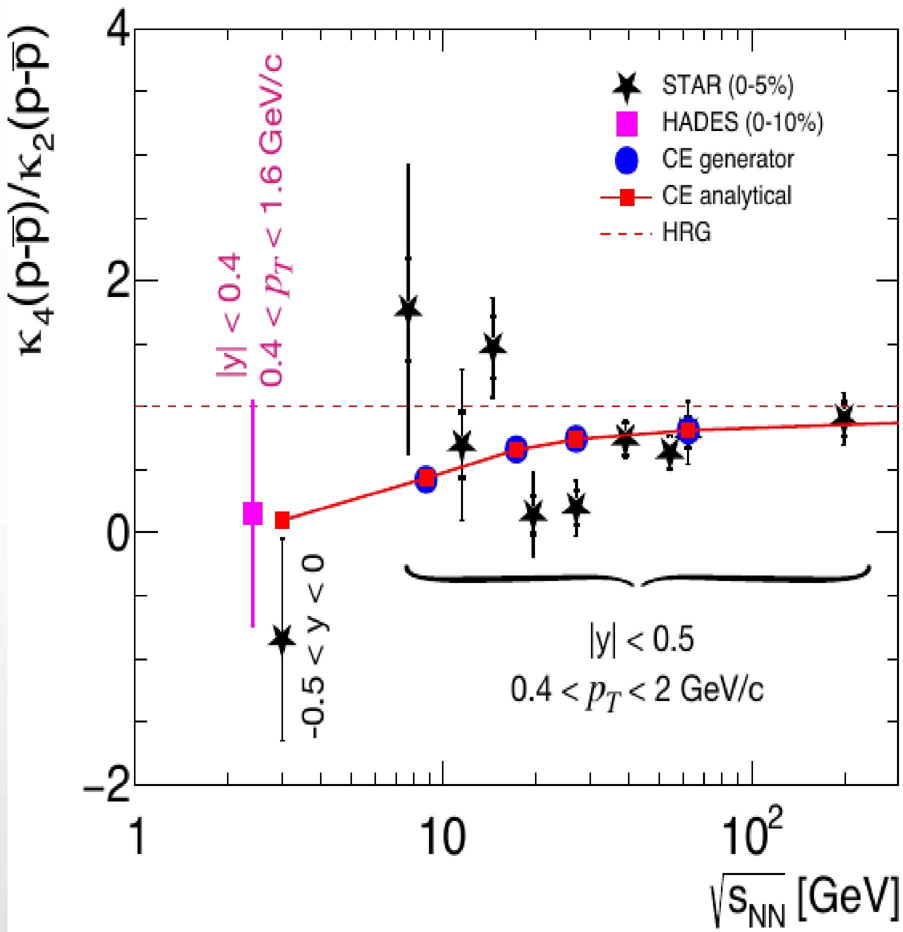

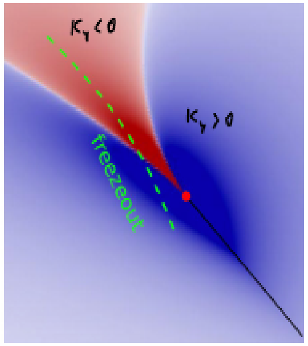

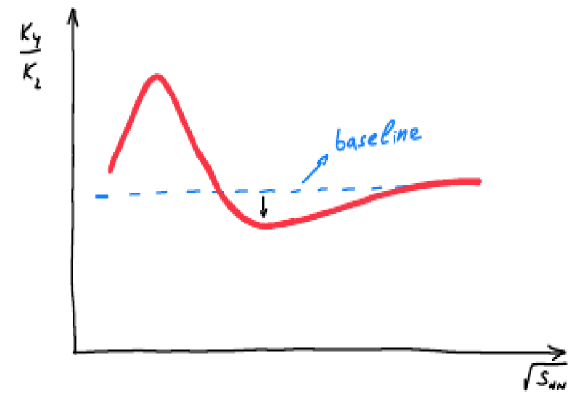

a dip in the excitation function is generic

M. Stephanov, PRL102.032301(2009), PRL107.052301(2011)
M.Cheng et al, PRD79.074505(2009)

STAR: Phys.Rev.Lett. 126 (2021) 9, 092301

non-monotonic behaviour with a significance of 3.1σ relative to Skellam expectation

CE Baseline: P. Braun-Munzinger, B. Friman, K. Redlich, AR, J. Stachel, NPA 1008 (2021) 12214

no statistically significant difference between the data and the canonical baseline (KS test: 1.2σ, χ^2 test: 1.5σ)

see also: V. Vovchenko, V. Koch, Ch. Shen, Phys.Rev.C 105 (2022) 1, 014904

higher statistics is needed for unambiguous conclusions

The energy excitation function of κ4 /κ2 of (net-)protons, within the experimental uncertainties, is consistent with the non-critical baseline (ideal gas + canonical Ensemble)   - Anar Rustamov (SQM 2022)

Experimental challenges in fluctuations measurements

Event-by-event identification issues

- Cut based approach
- Identity method
- PSET identity method

Non-dynamical contributions

- E-by-e fluctuations of wounded nucleons
- Depends on centrality selection methods

Contributions from pileup events

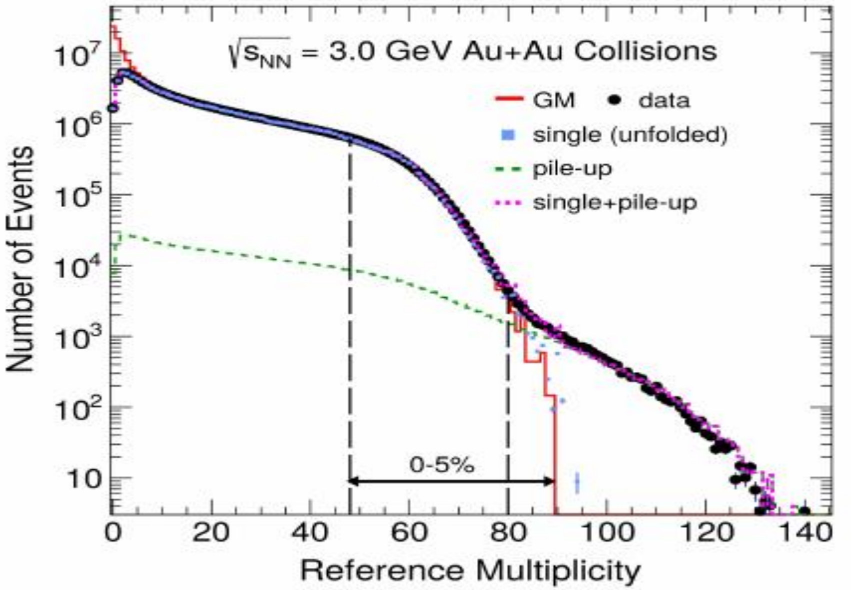

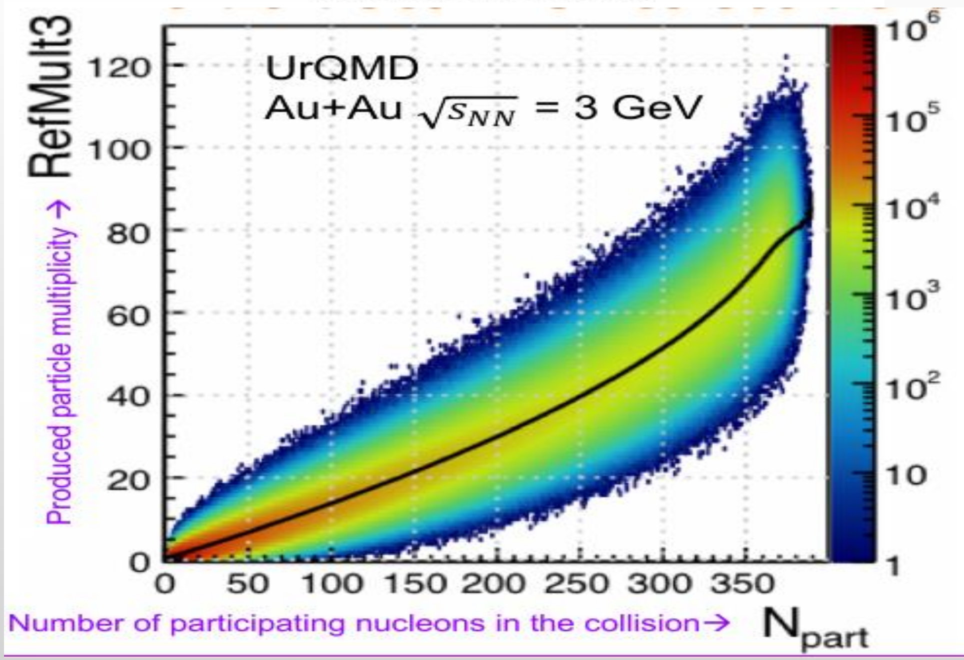

Finite-Size Effects and search for CEP

In HIC, both the size (**L**) and duration of formed system are finite.

Critical behavior changes with L

If the L is too small, the correlation length **ξ** can not be fully developed to cause a phase transition.

if the correlation length $\xi \sim |T - T_c|^{-\nu} \leq L$ the finite-size effect is not negligible and only a **pseudo-critical point, shifted from the genuine CEP, is observed.**

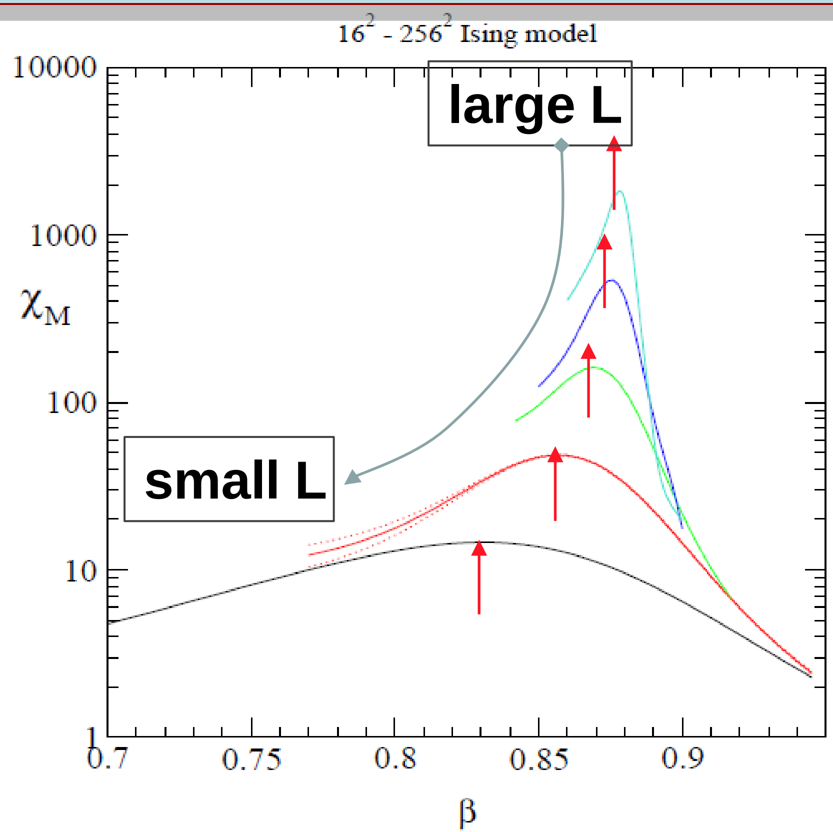

Note change in peak heights positions & widths with L

- ✓ **Finite-size effects have a specific dependencies on size (L)**
- ✓ **The scaling of these dependencies give access to the CEP's location, it's critical exponents and scaling function.**

Summary

- Preparation of the MPD detector and experimental program is ongoing, all activities are continued
- All components of the MPD 1-st stage detector are in advanced state of production
- Commissioning of the MPD Stage-I detector is expected in 2023
- Start of data t aking with BiBi@9.2 in 2024
- BM@N **first physics run with Xe+CsI ($\sqrt{s_{NN}}$ = 2.3-3.3 GeV) – October 2022**
- Further program will be driven by the physics demands and NICA capabilities

Booster

- Booster is fully assembled in the magnet yoke of the old synchrotron (solid basement, protection)
- First technical run – Dec 30th, 2020: He^{+} ions, energy up to 100 MeV/u
- Second run – Sep 6-24, 2021: total duration - about 450 h, He^{+} and $Fe14^{+}$ ions, energy up to 578 MeV/u, residual gas pressure in the beam pipe was sufficiently low for heavy ion acceleration
- The systems for the beam extraction from the Booster and transport line to the Nuclotron were put into operation and tuned, He^{+} and $Fe14^{+}$ beams were transported through the beam transfer line to Nuclotron

Booster assembled in the synchrotron magnet yoke

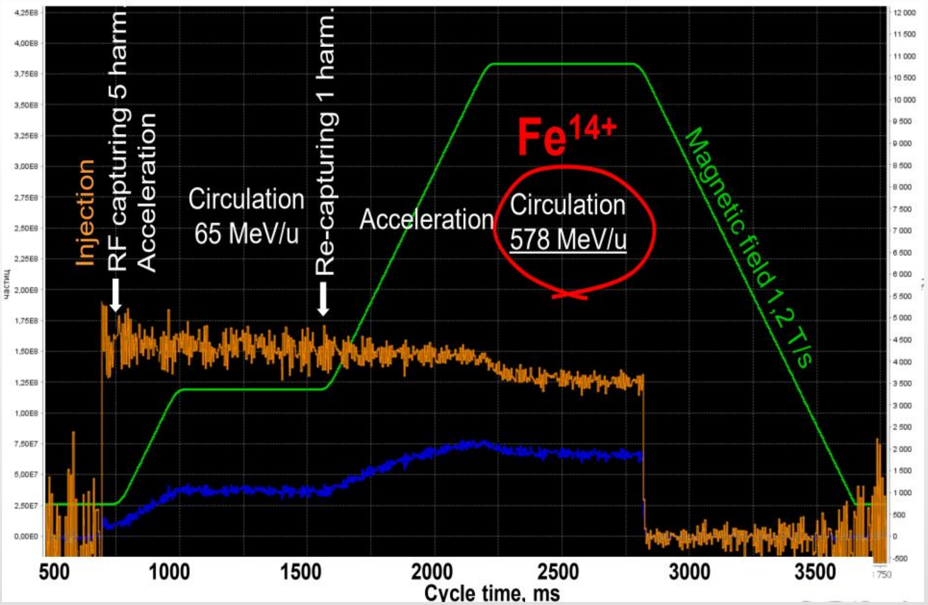

The beam was accelerated up to design energy of 578 MeV/u

First NICA run (Booster + Nuclotron)

- Duration: 2.01.2022 – 01.04.2022
- 3 GeV/u Carbon beam transported to BM@N area : 5.03 – 29.03
- 2150 h of the facility operation, BM@N stable operation with beams for 24 days
- SRC Collaboration collected 185 M events of carbon interactions with hydrogen target

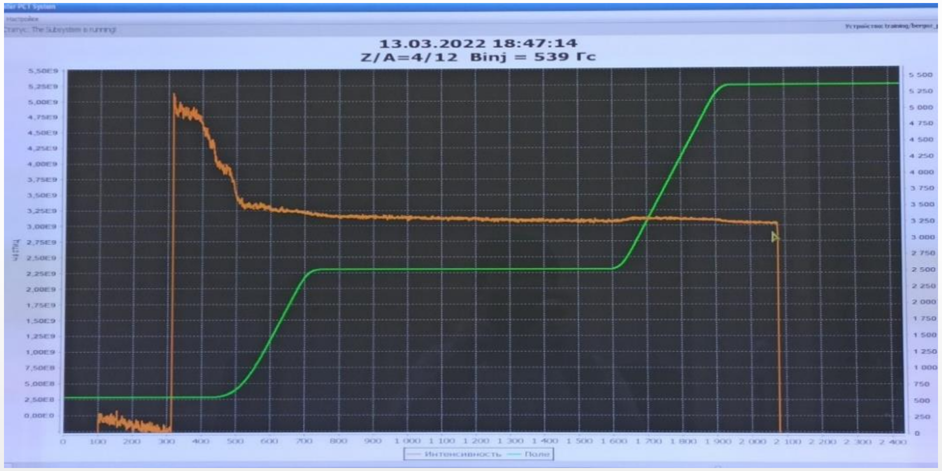

- Average efficiency ~ 30%
- Non-optimum stripping target thickness

Multi-Purpose Detector (MPD) Collaboration

MPD** International Collaboration was established in **2018
to construct, commission and operate the detector

10** Countries, **>450** participants, **31** Institutes and **JINR

Organization

Acting Spokesperson:	***Victor Riabov***
Deputy Spokesperson:	***Zebo Tang***
Institutional Board Chair:	***Alejandro Ayala***
Project Manager:	***Slava Golovatyuk***

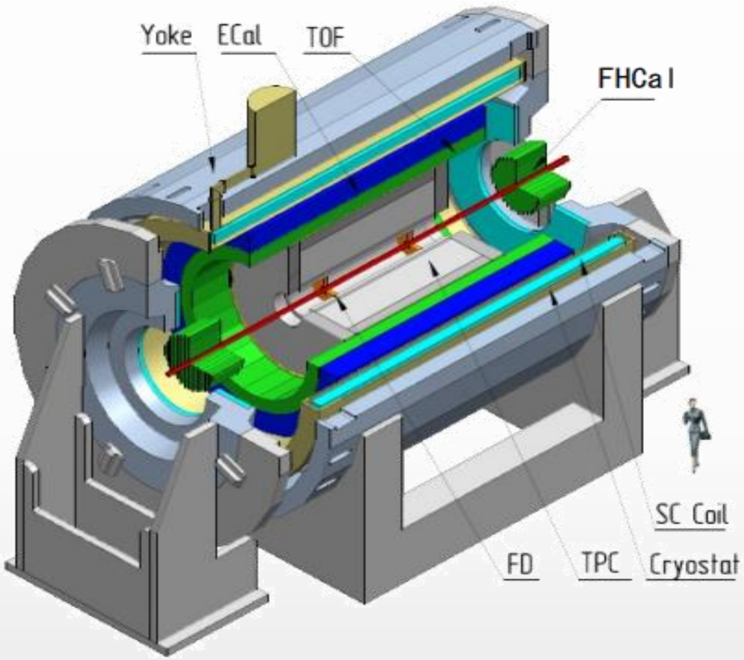

***Joint Institute for Nuclear Research**;*
*AANL, Yerevan, **Armenia;***
*University of Plovdiv, **Bulgaria;***
*Tsinghua University, Beijing, **China**;*
*USTC, Hefei, **China**;*
*Huzhou University, Huizhou, **China**;*
*Institute of Nuclear and Applied Physics, CAS, Shanghai, **China**;*
*Central China Normal University, **China**;*
*Shandong University, Shandong, **China**;*
*IHEP, Beijing, **China**;*
*University of South China, **China**;*
*Three Gorges University, **China**;*
*Institute of Modern Physics of CAS, Lanzhou, **China**;*
*Tbilisi State University, Tbilisi, **Georgia**;*
*FCFM-BUAP (Heber Zepeda) Puebla, **Mexico**;*
*FC-UCOL (Maria Elena Tejeda), Colima, **Mexico**;*
*FCFM-UAS (Isabel Dominguez), Culiacán, **Mexico**;*
*ICN-UNAM (Alejandro Ayala), Mexico City, **Mexico**;*
*Institute of Applied Physics, Chisinev, **Moldova**;*
*Institute of Physics and Technology, **Mongolia**;*

*Belgorod National Research University, **Russia**;*
*INR RAS, Moscow, **Russia**;*
*MEPhI, Moscow, **Russia**;*
*Moscow Institute of Science and Technology, **Russia**;*
*North Osetian State University, **Russia**;*
*NRC Kurchatov Institute, ITEP, **Russia**;*
*Kurchatov Institute, Moscow, **Russia**;*
*St. Petersburg State University, **Russia;***
*SINP, Moscow, **Russia**;*
*PNPI, Gatchina**, Russia**;*
*Vinča Institute of Nuclear Sciences**, Serbia**;*
*Pavol Jozef Šafárik University, Košice, **Slovakia***

MPD Hall

- MPD hall is available for detector activities
- Installation of the MPD superconducting coil inside the magnet yoke - 29 July, 2021, followed by alignment of cold mass, pressure test of thermal shield and cryostat cold mass, replacement of flanges, vacuum test of solenoid vessel, leak test of cryostat
- Ongoing: temperature probes cables, assembling magnet yoke, alignment, installation of top platform, chimney installation, cryogenic system with control systems, magnetic field measurement

Trigger system

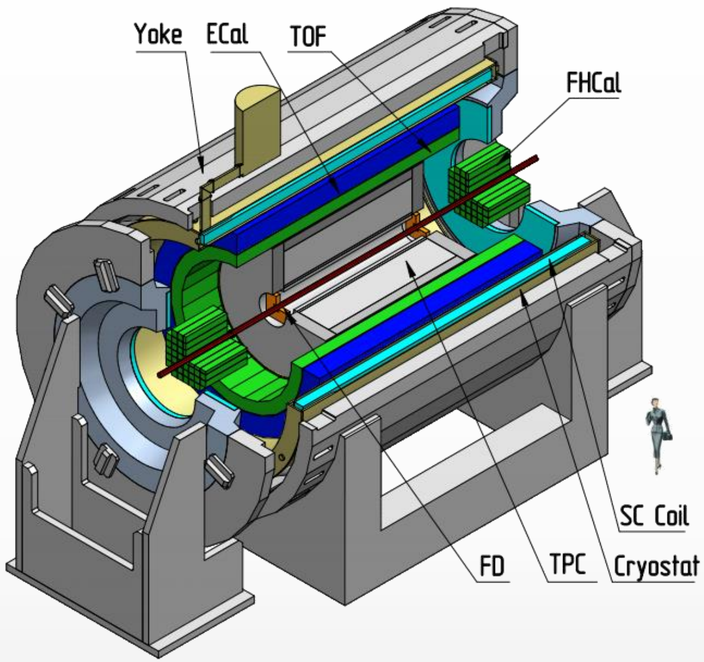

- FFD (Fast Forward Detector):
  - ✓ fast event triggering
  - ✓ T_0 for time measurements in the TOF and ECAL

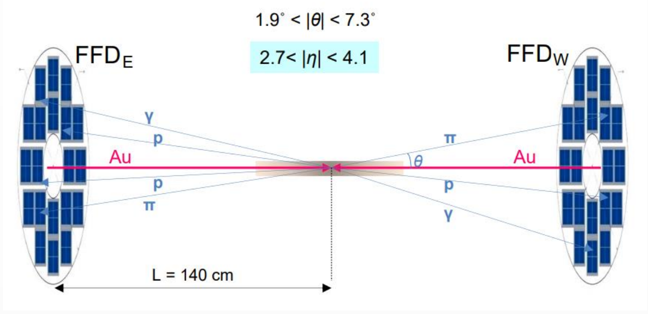

- FHCAL (Forward Hadron Calorimeter) – detector for event centrality and reaction plane measurements with potential for event triggering

- MPD challenges at NICA energies:
  - ✓ low multiplicity of particles produced in heavy-ion collisions
  - ✓ particles are not ultra-relativistic (even the spectator protons)
- Forward detectors are in advanced state of production (electronics and integration)

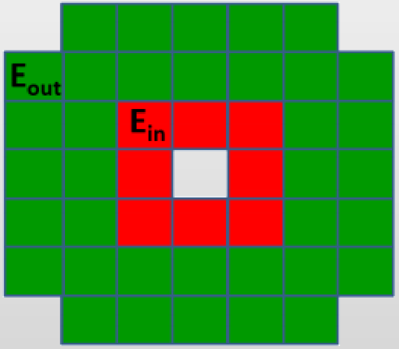

$2 < |\eta| < 5$

$\sim 1\text{x}1\ \text{m}^2$

Trigger efficiency vs. z-vertex

DCM-QGSM-SMM, BiBi@9.2

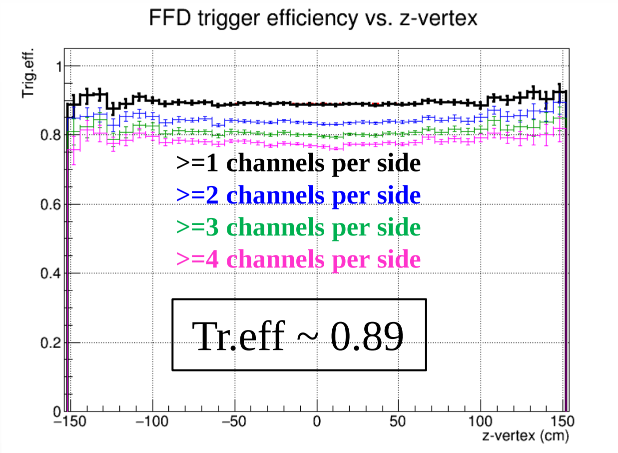

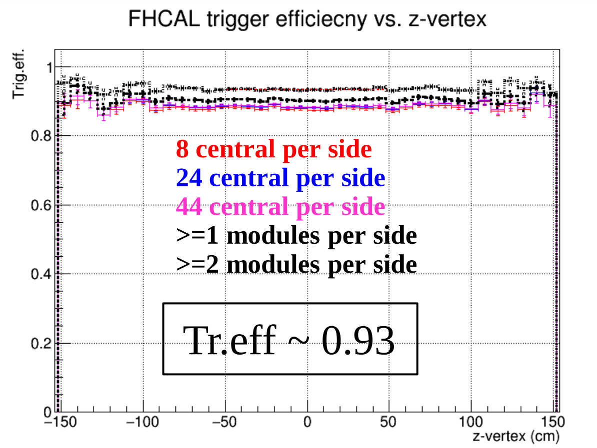

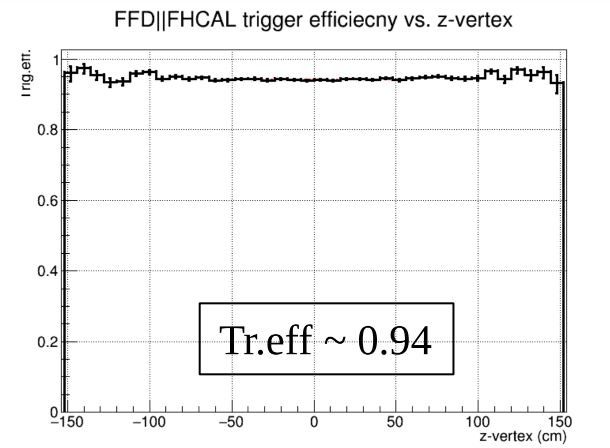

PHQMD, BiBi@9.2

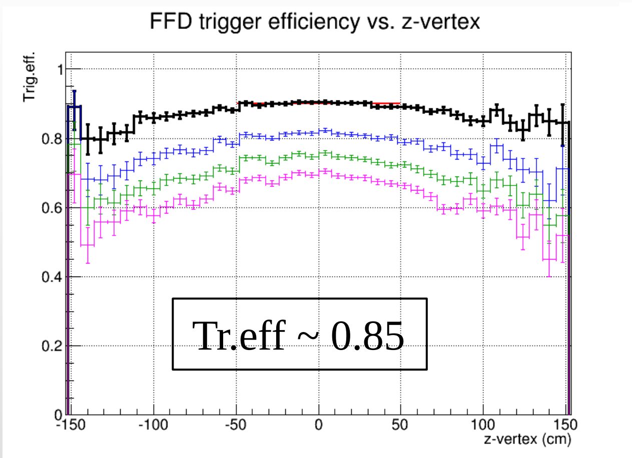

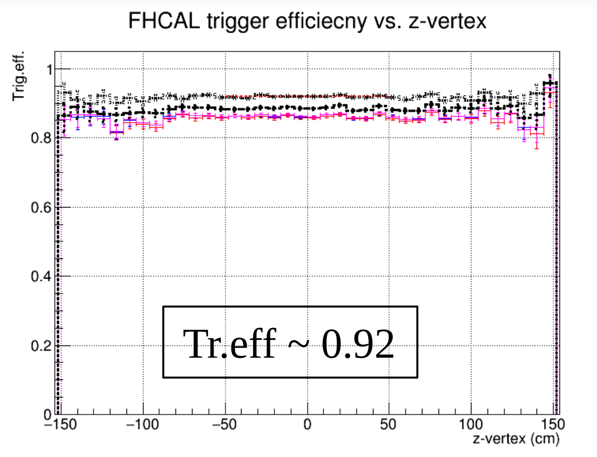

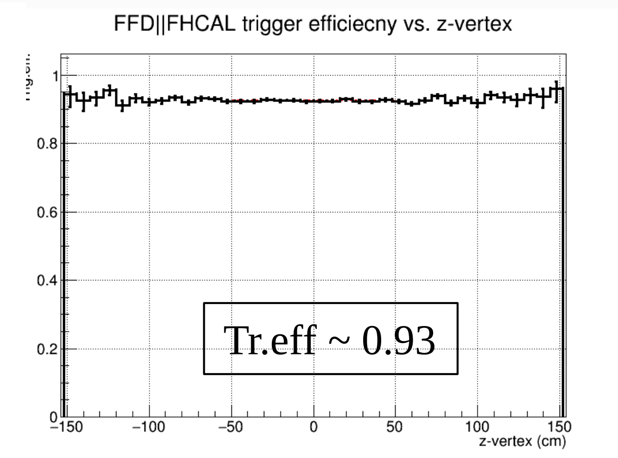

- Efficiency is 80-95% in different trigger configuration; approximately the same numbers for two generators
- FFD efficiency shows z-vertex dependence for PHQMD; FHCAL and FFD||FHCAL does not

Centrality studies by TPC

- AuAu@7.7 GeV (UrQMD), reconstructed data
- **MC Glauber (MC-Gl)** and **Bayesian inversion method (Γ-fit)** methods for extraction of b

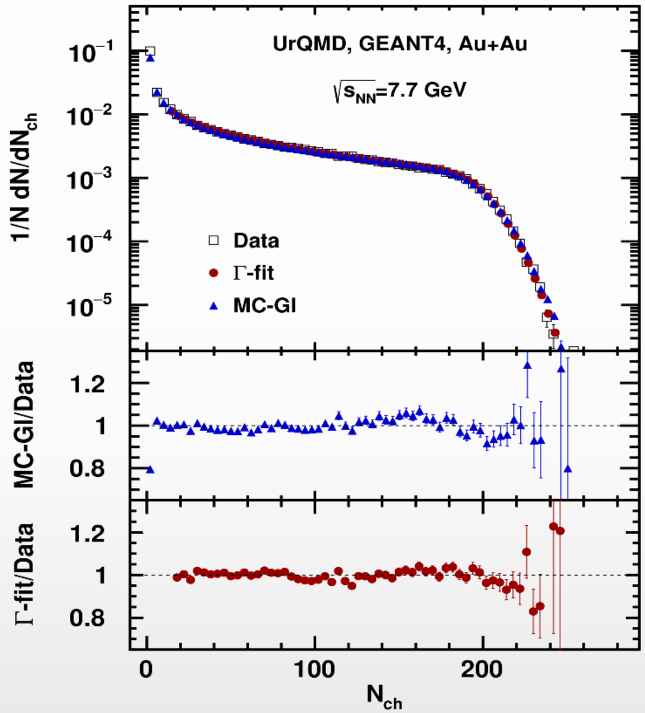

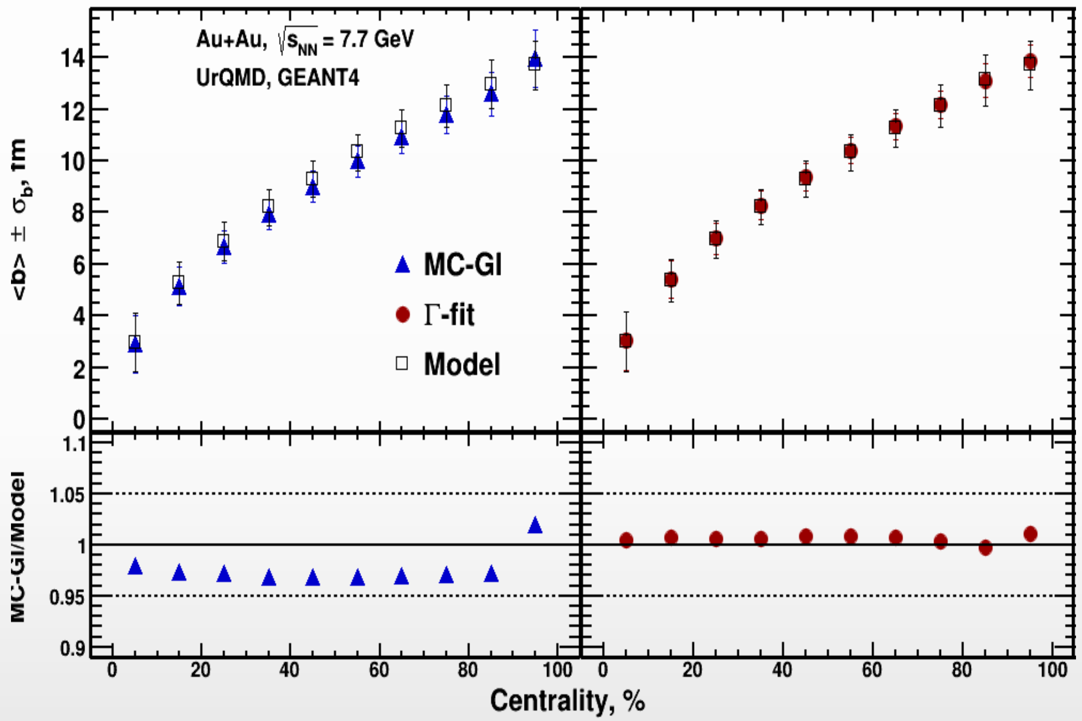

- Comparable results with PHSD and SMASH event generators at different energies → robust method
- Centrality estimation consistent with STAR → good for cross-checks between the experiments
- Centrality measurements are possible in a wide |z-vertex| < 120 cm range

[1] Centrality Determination in Heavy-ion Collisions with MPD Detector at NICA, Acta Physica Polonica B 14 (2021) 3, 503-506
[2] Relating Charged Particle Multiplicity to Impact Parameter in Heavy-Ion Collisions at NICA Energies, Particles 4 (2021) 2, 275-287

NICA

Identified hadron spectra

- Particle spectra, yields and ratios probe bulk properties of the firerball and flow
- Advantage of the MPD is in large and uniform acceptance, excellent PID capabilities using combined analysis of TPC (dE/dx) and TOF signals

- 0-5% central AuAu@9 GeV (PHSD, with partonic phase and chiral symmetry restoration effects):

Phys.Part.Nucl. 53 (2022) 2, 203-206

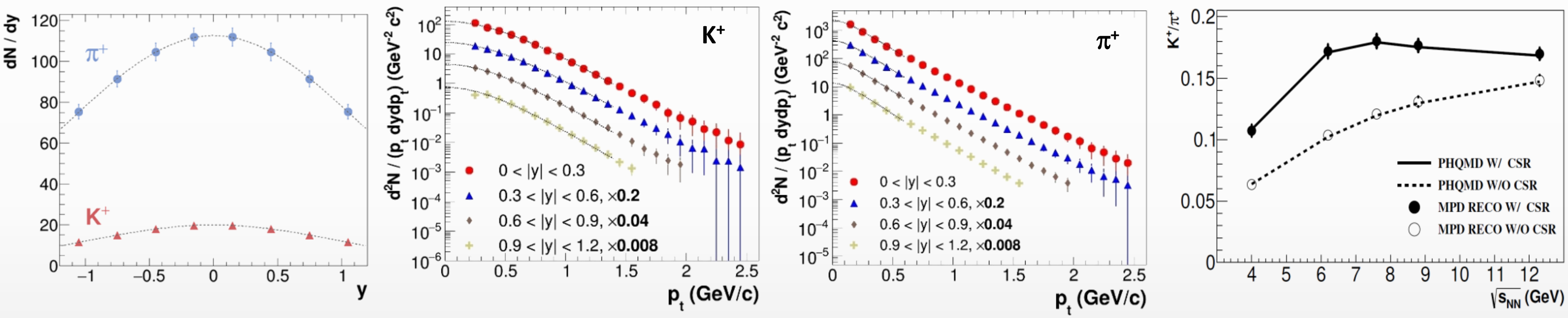

✓ MPD samples ~ 70% of the π/K/p production in the full phase space

✓ hadron spectra are measured from 0.2 MeV/c to 2.5 GeV/c in transverse momentum with the TPC&TOF

✓ unmeasured hadron yields at low p_T and large values of rapidity can be extracted from extrapolation of the measured spectra (B-W for p_T spectra and Gaussian for rapidity spectra in exampled above)

- Ability to cover full energy range of the “horn” with consistent acceptance across different collision systems and collision energies

Weak decays of strange baryons - I

- Strangeness production probes the EoS, phase boundaries and onset of deconfinement
- Antibaryon-to-baryon ratios at intermediate momenta are sensitive to CEP (a falling trend in contrast to a constant behavior in the scenario without CEP)
- AuAu@11 GeV (PHSD):

Acta Physica Polonica B 14 (2021) 3, 529-532

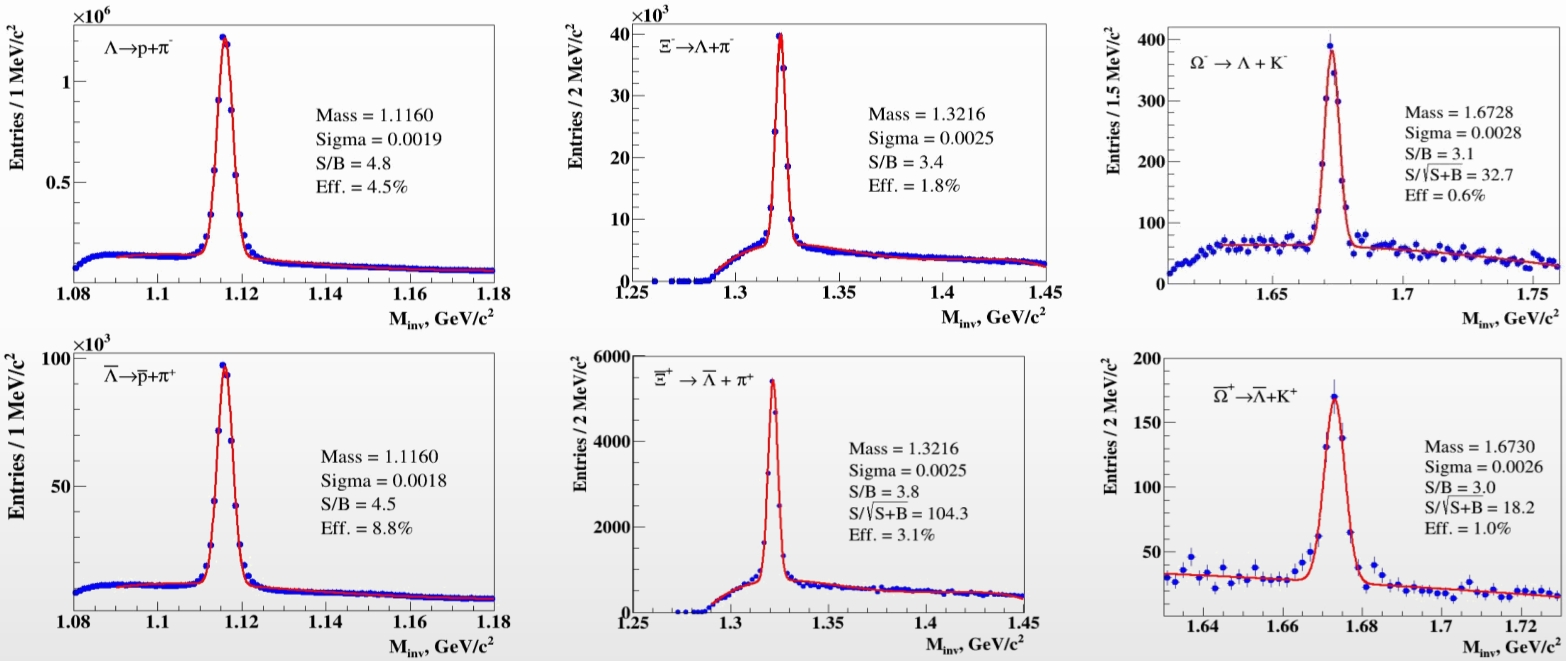

- ✓ Strange baryons can be reconstructed with good S/B ratios using charged hadron identification in the TPC&TOF and different decay topology selections
- ✓ Relative yields of the baryons for ~ 500 M sampled events:

Λ	anti-Λ	Ξ^-	anti-Ξ^+	Ω^-	anti-Ω^+
$3 \cdot 10^8$	$3.5 \cdot 10^6$	$1.5 \cdot 10^6$	$8.0 \cdot 10^4$	$7 \cdot 10^4$	$1.5 \cdot 10^4$

More hypernuclei

- Information on YN interactions, strange sector of nuclear EoS, astrophysics
- BiBi@9.2 GeV (PHQMD):

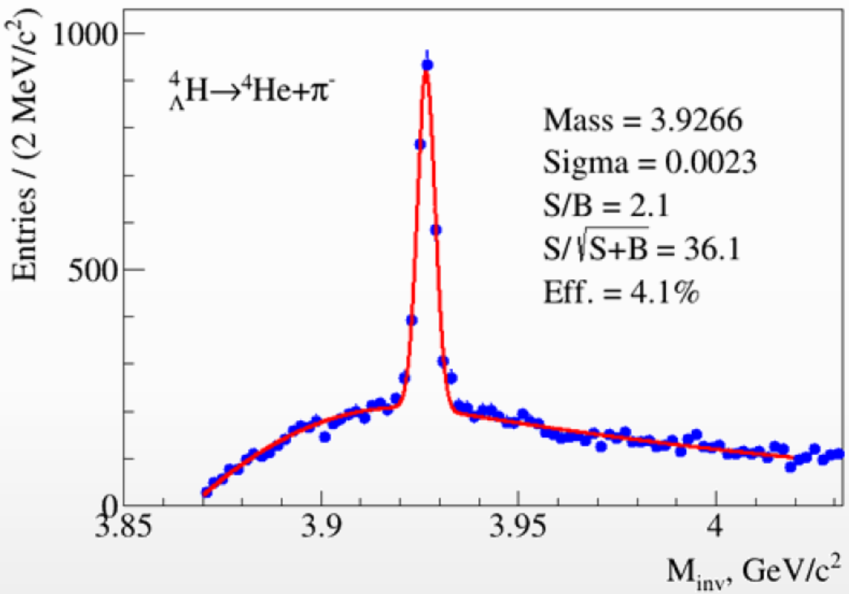

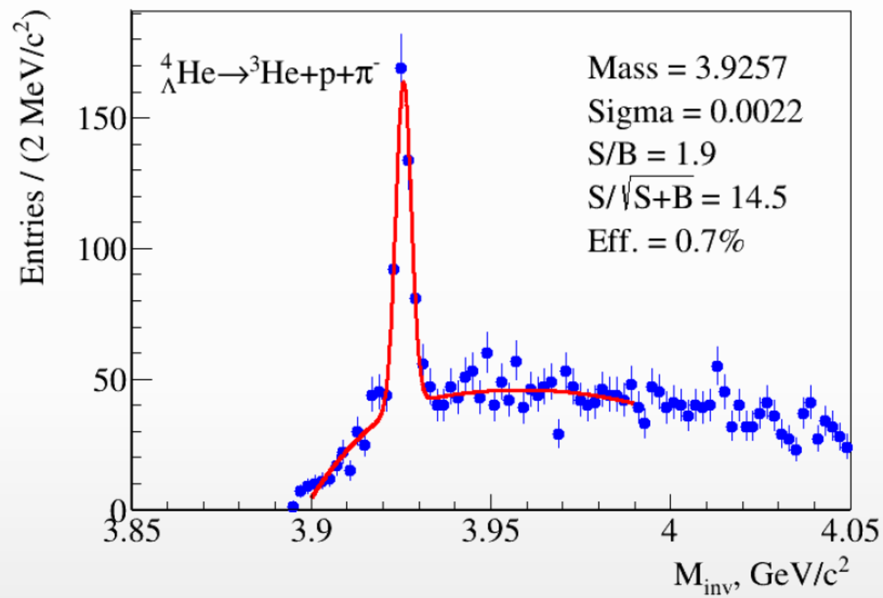

- The Monte Carlo event sample was enriched by hypernuclei distributed according to the η-p_T phase space predicted by the PHQMD generator
- Signals for heavier hypernuclei can be seen with the equivalent statistics of ~140 M events

Higher harmonics (v_3)

- Models show that higher harmonic ripples are more sensitive to the existence of a QGP phase
- In models, v_3 goes away when the QGP phase disappears????
- 15 M of reconstructed vHLLE + UrQMD events for AuAu@11.5 GeV

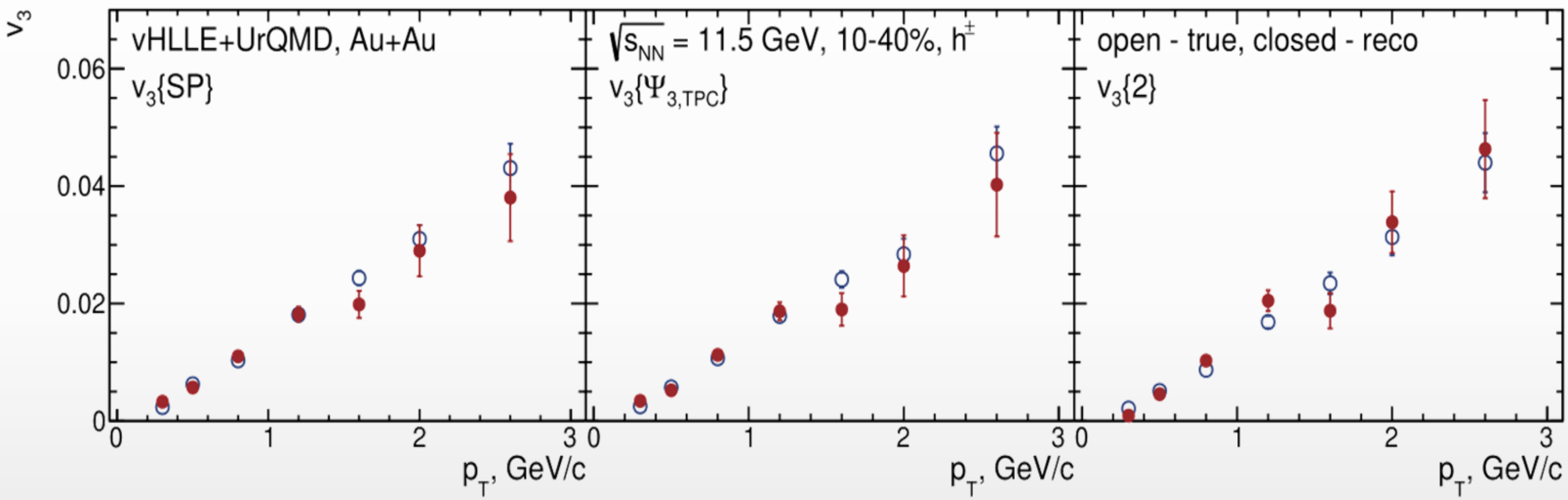

- Reconstructed and generated v_3 of charged hadrons are in good agreement for all methods

BACKUP

Accelerator Complex in Dubna

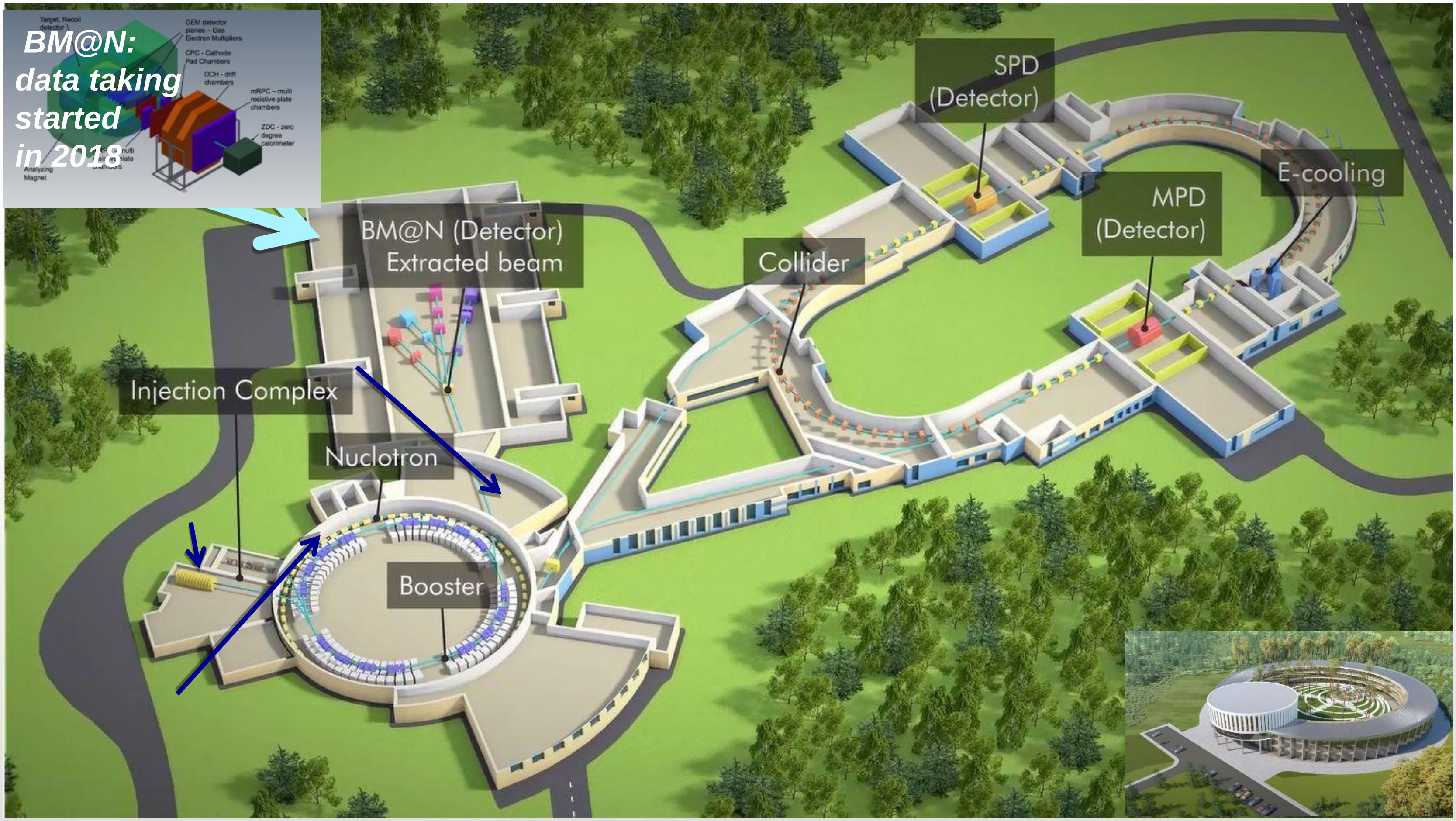

- ❖ Budget ~ 500 M$
- ❖ First collisions in collider – end of 2023

STAR ☆

$\sqrt{s_{NN}}$ (GeV)	Beam Energy (GeV/nucleon)	Collider or Fixed Target	$y_{center\ of\ mass}$	μ_B (MeV)	Run Time (days)	No. Events Collected (Request)	Date Collected
200	100	C	0	25	2.0	138 M (140 M)	Run-19
27	13.5	C	0	156	24	555 M (700 M)	Run-18
19.6	9.8	C	0	206	36	582 M (400 M)	Run-19
17.3	8.65	C	0	230	14	256 M (250 M)	Run-21
14.6	7.3	C	0	262	60	324 M (310 M)	Run-19
13.7	100	FXT	2.69	276	0.5	52 M (50 M)	Run-21
11.5	5.75	C	0	316	54	235 M (230 M)	Run-20
11.5	70	FXT	2.51	316	0.5	50 M (50 M)	Run-21
9.2	4.59	C	0	372	102	162 M (160 M)	Run-20+20b
9.2	44.5	FXT	2.28	372	0.5	50 M (50 M)	Run-21
7.7	3.85	C	0	420	90	100 M (100 M)	Run-21
7.7	31.2	FXT	2.10	420	0.5+1.0+ scattered	50 M + 112 M + 100 M (100 M)	Run-19+20+21
7.2	26.5	FXT	2.02	443	2+Parasitic with CEC	155 M + 317 M	Run-18+20
6.2	19.5	FXT	1.87	487	1.4	118 M (100 M)	Run-20
5.2	13.5	FXT	1.68	541	1.0	103 M (100 M)	Run-20
4.5	9.8	FXT	1.52	589	0.9	108 M (100 M)	Run-20
3.9	7.3	FXT	1.37	633	1.1	117 M (100 M)	Run-20
3.5	5.75	FXT	1.25	666	0.9	116 M (100 M)	Run-20
3.2	4.59	FXT	1.13	699	2.0	200 M (200 M)	Run-19
3.0	3.85	FXT	1.05	721	4.6	259 M -> 2B(100 M -> 2B)	Run-18+21

5

(Di)electrons

- ❖ Dielectron spectra are sensitive probes of the deconfinement and the chiral symmetry restoration
- ❖ AuAu@11 GeV (UrQMD for background & PHQMD for signal)

$n \cdot \sigma_e^{TPC}$ with $2\sigma_e$ PID in the TOF

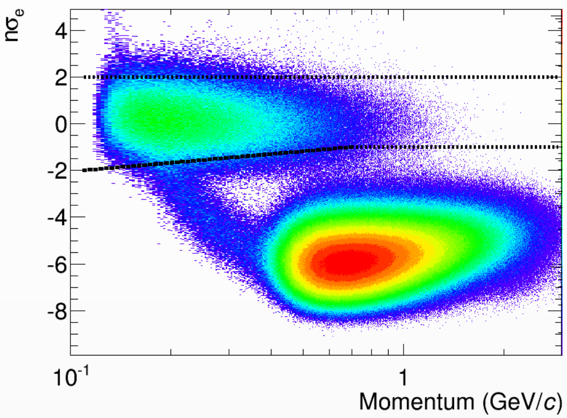

Efficiency of e-track reconstruction

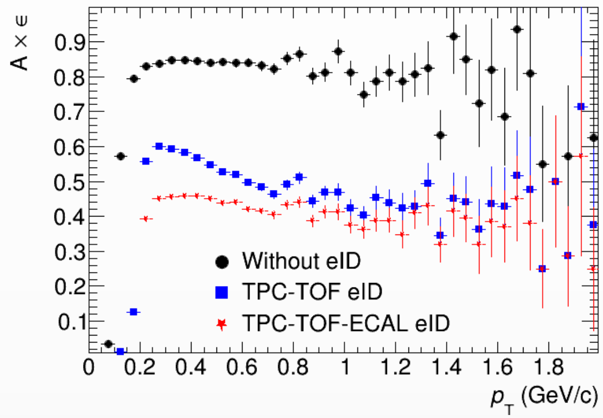

Electron purity

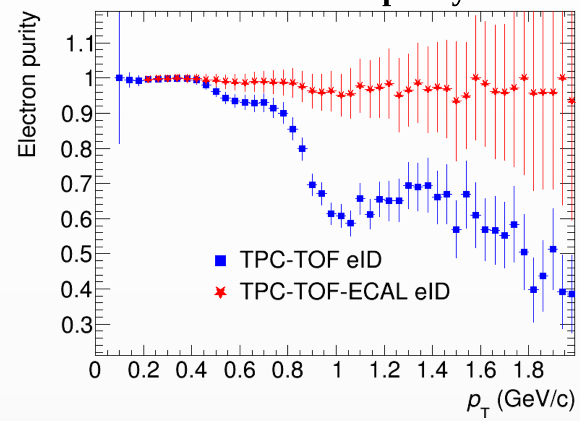

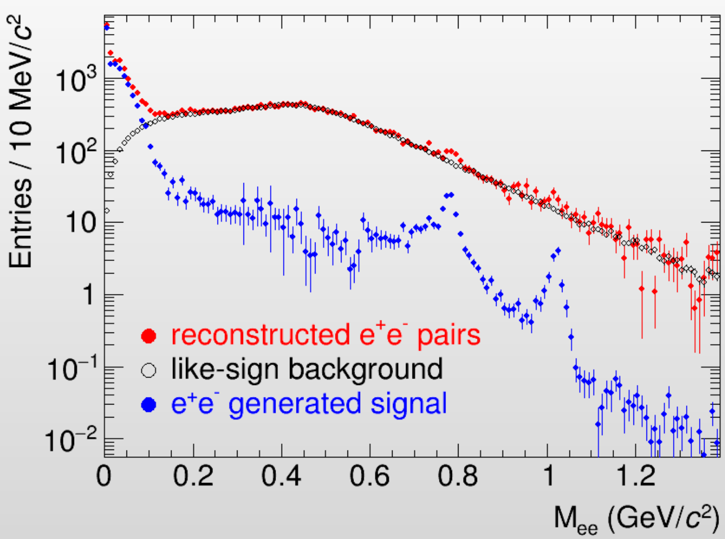

- ❖ S/B (integrated in 0.2-1.5 GeV/c^2) ~ 5-10%
- ❖ Methods to improve S/B ratio while preserving reasonable efficiency for the pairs are being developed and matured

Support Frame for detectors inside of the Solenoid

The structure of Support Frame is made of carbon fiber which allows for deformation less than 3 mm under load with detectors (~80 T).
Producer - The Central Research Institute for Special Machinery, Khotkovo, Moscow region is a leading Russian enterprise in design and production of structures on the basis of advanced polymer composite materials for rocket & space engineering, transport, power, petrochemical machinery and other industries.

- the Frame will be transported to Dubna in November 2021
- December 2021 (as soon as Magnetic field measurements is finished)
- Representatives of the Company will participate in the process of installation of Support Frame into MPD and its alignment

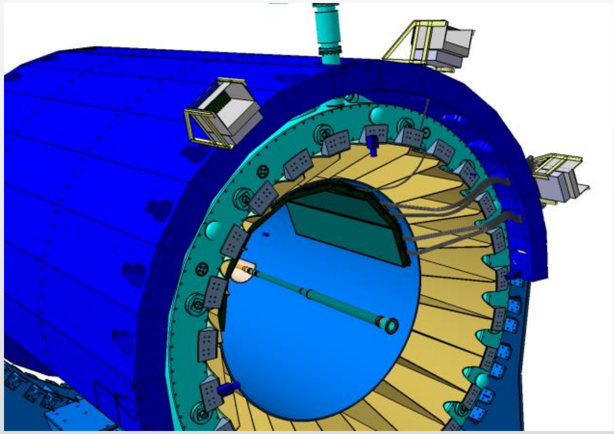

Time Projection Chamber (TPC): main tracker

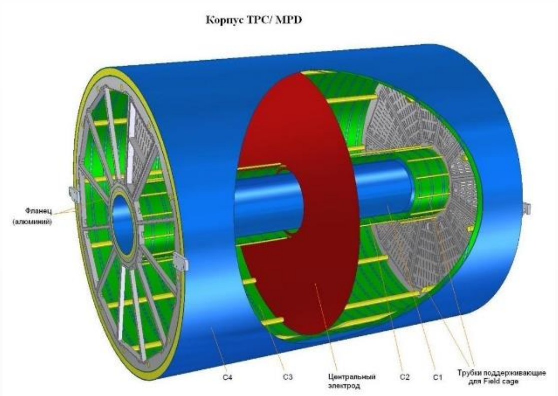

length	*340 см*
outer Radii	*140 см*
inner Radii	*27 см*
gas	*90%Ar+10%CH_4*
drift velocity	*5.45 см / μs;*
drift time	*< 30 μs;*
# R-O chamb.	*12 + 12*
# pads/ chan.	***95 232***
max rate	*< 7kGz (L= 10^{27})*

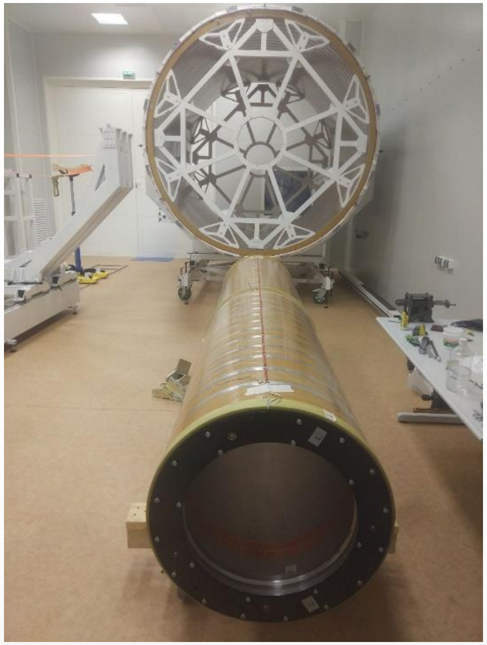

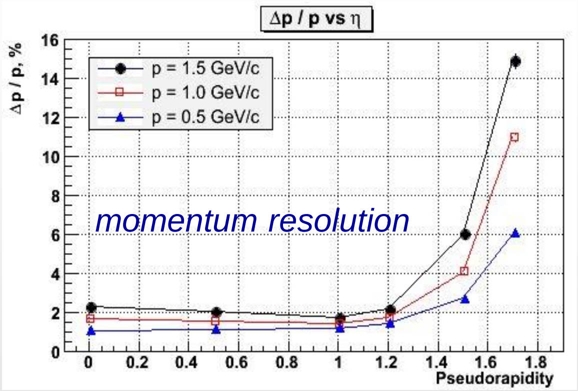

r-o chamber

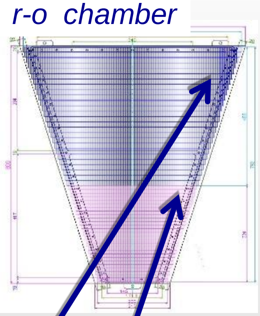

FE electronics: **FEC64SAM** –
*dual **SAMPA** card (**ALICE** technology)*

pad structure:
- *rows – 53*
- *large pads 5 × 18 mm^2*
-

Read-Out Chambers (ROCs) are ready and tested (production at JINR)
113 Electronics sets (8%) produced
Two sites (Moscow, Minsk) tested for electronics production
C1-C2 and C3-C4 cylinders assembled
TPC flange under finalization

MPD Time-of-Flight

Mass production staff: 4 physicists, 4 technicians, 2 electronics engineers
Productivity: ~ 1 detector per day (1 module/2 weeks)


Glass cleaning with ultrasonic wave & deionized water


Automatic painting of the conductive layer on the glass


MRPC assembling


Soldering HV connector and readout pins

All procedure of detector assembling and optical control is performed in a clean rooms ISO class 6-7.

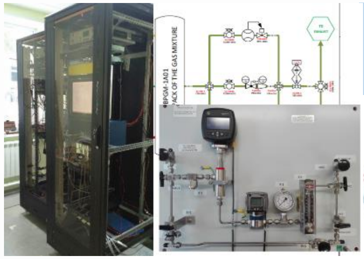
TOF gas system: Responsibility of the Polish group (WUT)

Dimensions of sensitive area 600 x300 mm^2

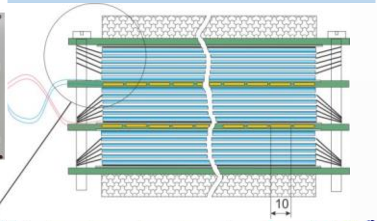

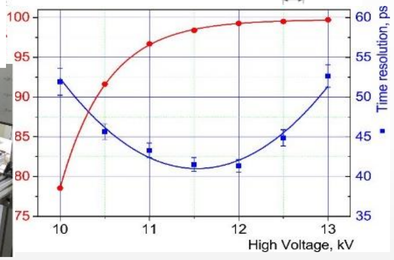

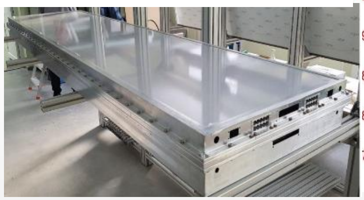

Single detector time resolution: 50ps

	Number of detectors	Number of readout strips	Sensitive area, m^2	Number of FEE cards	Number of FEE channels
MRPC	1	24	0.192	2	48
Module	10	240	1.848	20	480
Barrel	280	6720	51.8	560	**13440** (1680 chips)

Purchasing of all detector materials completed
So far 40% of all MRPCs are assembled
Assembled half sectors of TOF are under Cosmics tests
Investigation of solutions for detector integration and technical installations

Electromagnetic Calorimeter (ECAL)

- ❖ *Pb+Sc "Shashlyk"* — *read-out: WLS fibers + MAPD* — *L ~35 cm (~ 14 X_0)*
- ❖ *Segmentation (4x4 cm^2)* — *σ(E) better than 5% @ 1 GeV* — *time resolution ~500 ps*

Barrel ECAL = <u>38400</u> ECAL towers (2x25 half-sectors x 6x8 modules/half-sector x 16 towers/module)

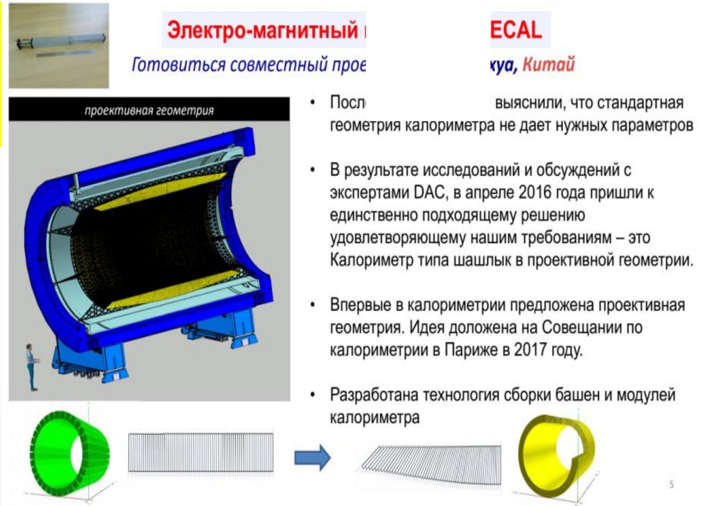

Projective geometry

So far ~300 modules (16 towers each) = 3 sectors are produced
Another 3 sectors are planned to be completed by May 2021
Chinese collaborators will produce 8 sectors by the end of 2021
25% of all modules are produced by JINR (production area in Protvino) 75% produced in China, currently funding is secured for approx. 25%

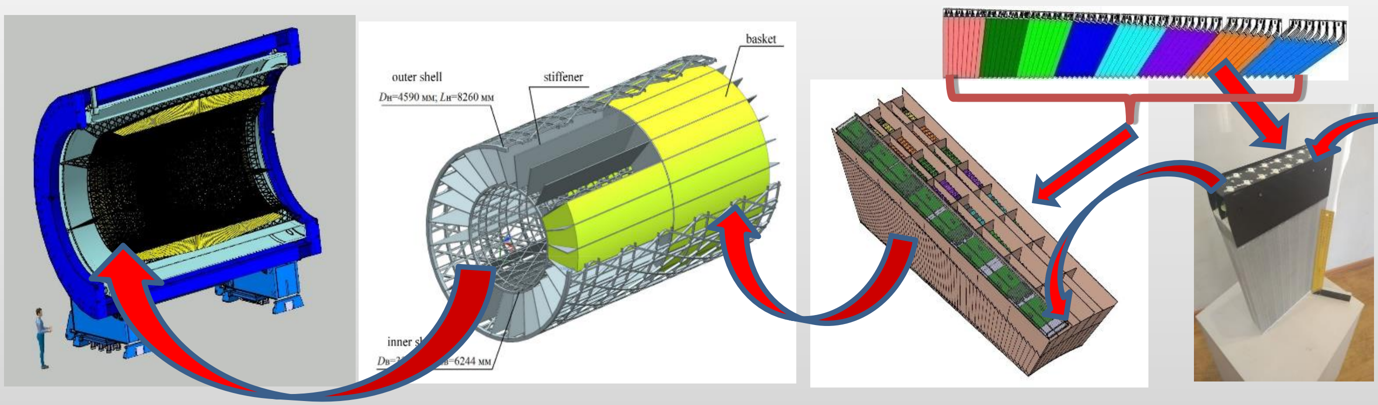

Sectors in dedicated Containers

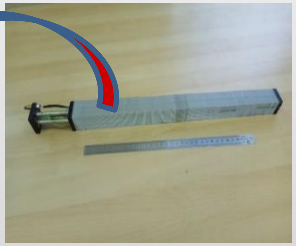

Photo of one tower

Forward Hadron Calorimeter (FHCal)

- **All (90+spare) FHCal modules are assembled and are used for the tests.**
- **100 Front-End-Electronics (FEE) boards are produced and tested.**

The activities with modules:

- **Tests with cosmic muons;**
- **Tests of Front-End-Electronics (FEE);**
- **Study of FEE electronic noises;**
- **Development of FHCal trigger;**
- **Development of Slow Control.**

FHCal Trigger efficiency

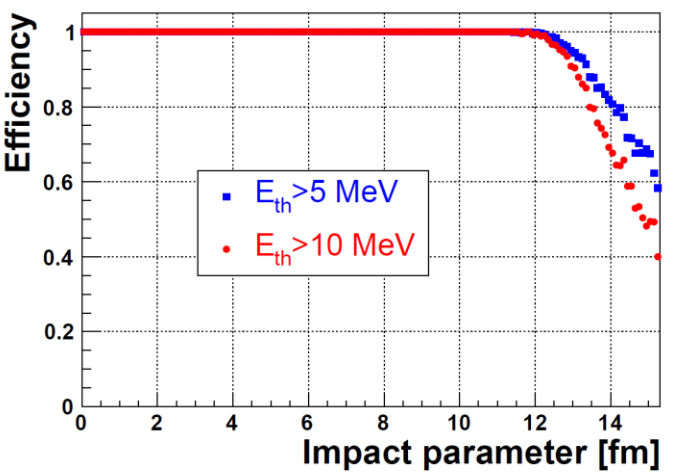

FHCal energy calibration with cosmic

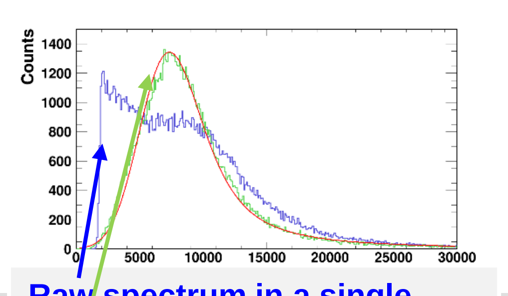

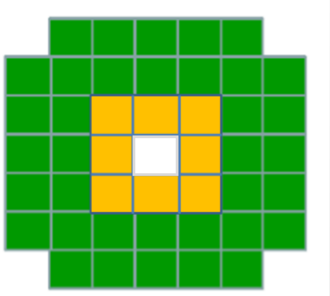

Raw spectrum in a single

Corrected to the pass length in scintillators

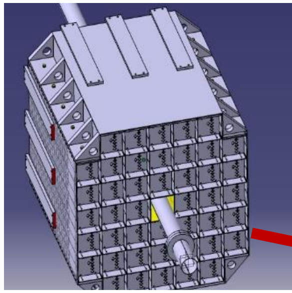

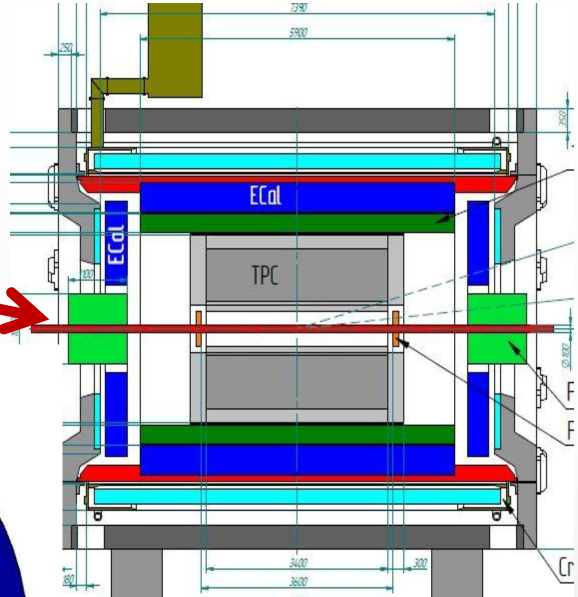

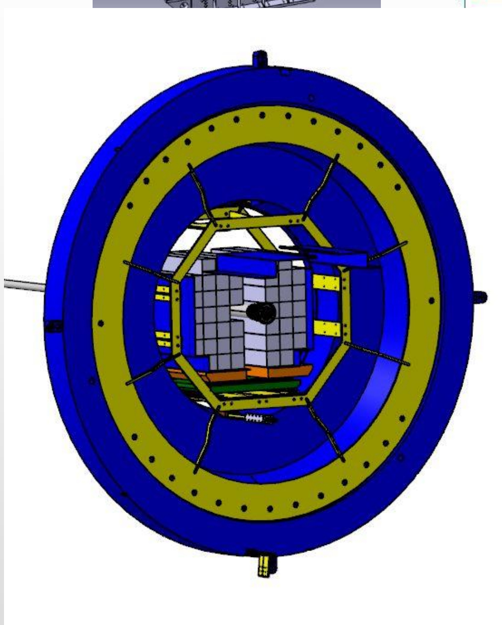

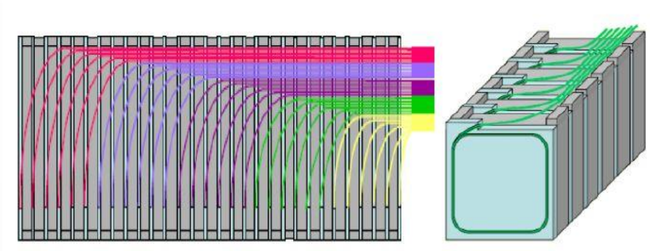

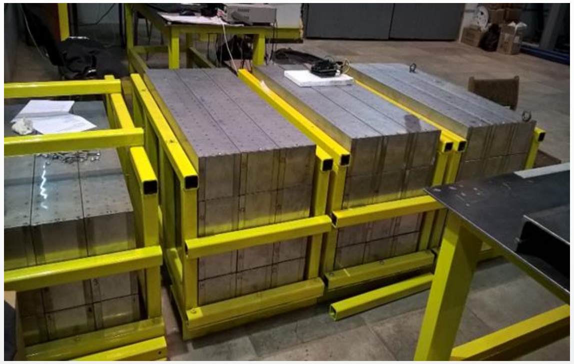

- Two-arms at ~3.2 m from the interaction point.
- Each arm consists of 44 individual modules.
- Module size 150x150x1100cm^3 (42 layers)
- Pb(16mm)+Scint.(4mm) sandwich
- 7 longitudinal sections
- 6 WLS-fiber/MAPD per section
- 7 MAPDs/module

FFD - Fast Trigger L_0 for MPD

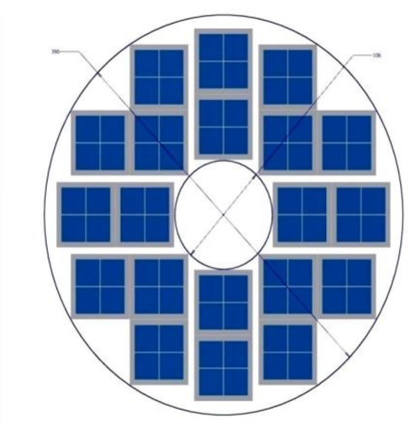

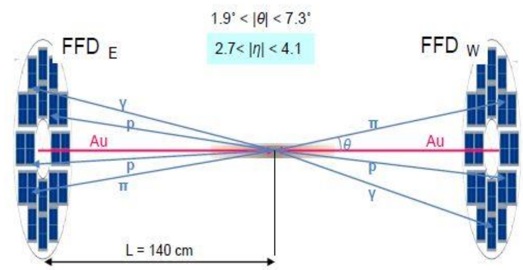

FFD provides information on
- interaction rate (luminosity adjustment)
- bunch crossing region position

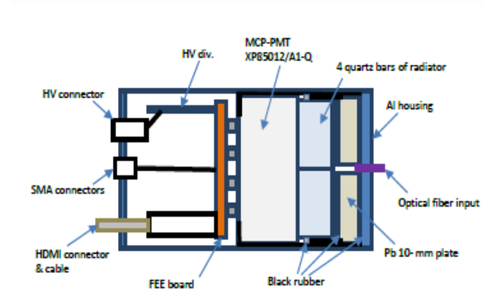

Fig. 4-1. A scheme of the FFD module.

15 mm quartz radiator
10 mm Lead converter

The FFD sub-detector consists of
20 modules based on
Planacon multianode MCP-PMTs
80 independent channels

MPD trigger group is created on the basis of FFD team
Beside FFD we consider the signals from FHCal to be implemented into trigger L0
The FHCal team have produced trigger electronics.
Monte Carlo studies will be used to optimize the properties of the L0 trigger

Simulation setup

- ✓ UrQMD v3.4 with hybrid model (3+1d hydro, **bag model** EoS, hadronic rescattering and resonances within UrQMD)
- ✓ π^0 and decay photon spectrum are calculated **within the same simulation**
- ✓ impact parameter range 0<b<9 fm
- ✓ In hydrodynamical evolution, for each volume we calculate thermal gamma yield based on T, energy density (e), QGP fraction, baryonic chemical potential. We integrate these yields over time (until freeze-out time) and space.
- ✓ Two extreme cases: calculate thermal gamma emission from the volume above freeze-out criterion ($e > e_{freezeout}$), or calculate for all volumes. Reality somewhere in between (all volumes interact during hydro evolution). Comparing these options one can estimate theoretical uncertainties

$$\frac{d^3 N^{\gamma,therm}}{dy\, d^2 k_T} = \int_{\Omega} dV\, dt\, R_{\gamma}\left(k, T(x), \mu(x), u(x)\right)$$

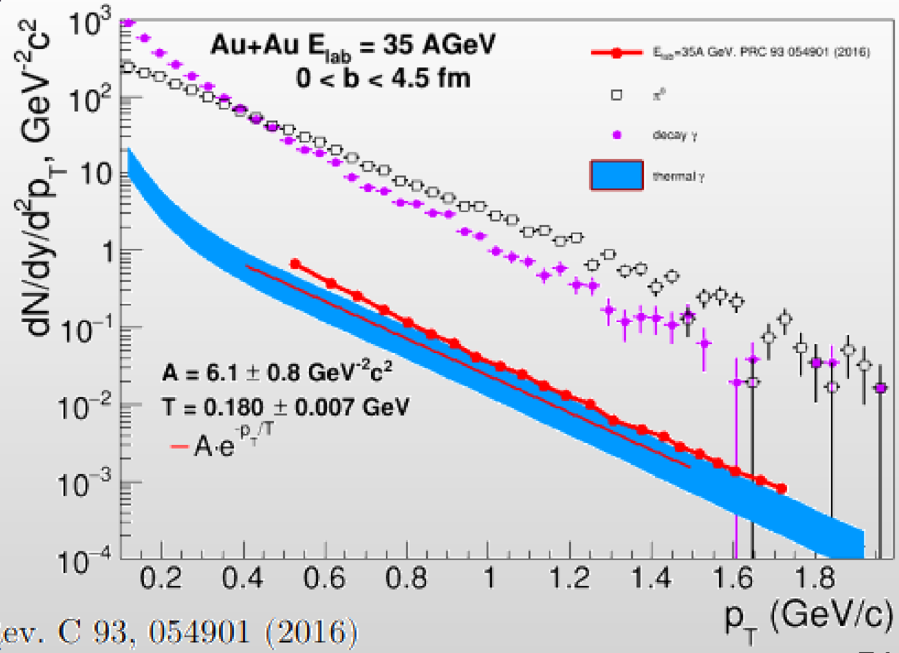

Why simulations in PRC 93 054901 (2016) and PRC 81 044904 (2010) have almost the same yield despite ~5 times difference in energy (35 vs 158 AGeV)?

Comparison with S. Endres, H. van Hees, M. Bleicher, Phys. Rev. C 93, 054901 (2016)

The Bayesian inversion method (Γ-fit): main assumptions

- Relation between multiplicity N_{ch} and impact parameter b is defined by the fluctuation kernel:

$$P(N_{ch}|c_b) = \frac{1}{\Gamma(k(c_b))\theta^k} N_{ch}^{k(c_b)-1} e^{-n/\theta}$$

c_b – impact parameter based centrality

$$c_b = \frac{1}{\sigma_{inel}} \int_0^b P_{inel}(b') 2\pi b' db' \simeq \frac{\pi b^2}{\sigma_{inel}}$$

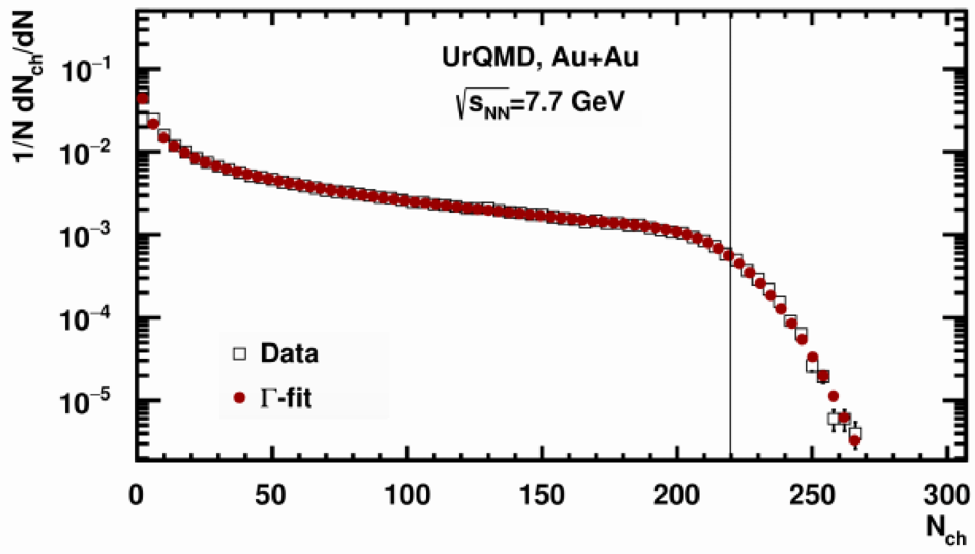

σ_{inel} – geometrical inelastic NN cross section

$P_{inel}(b)$ – probability of inelastic NN collision ($P_{inel}(b) \approx 1$)

R. Rogly, G. Giacalone and J. Y. Ollitrault, Phys.Rev. C98 (2018) no.2, 024902

Implementation in MPD: https://github.com/Dim23/GammaFit

Two particle correlations

- Femtoscopy is used in heavy-ion collision to determine the size of the particle-emitting region and space-time evolution of the produced system.
- Measurement for pions are straightforward and robust, large discovery potential in correlations for kaons and protons, as well as correlations including hyperons

AuAu@7.7 GeV (vHLLE), extracted 3D pion radii versus m_T vs. STAR data (PRC 96, 024911(2017))

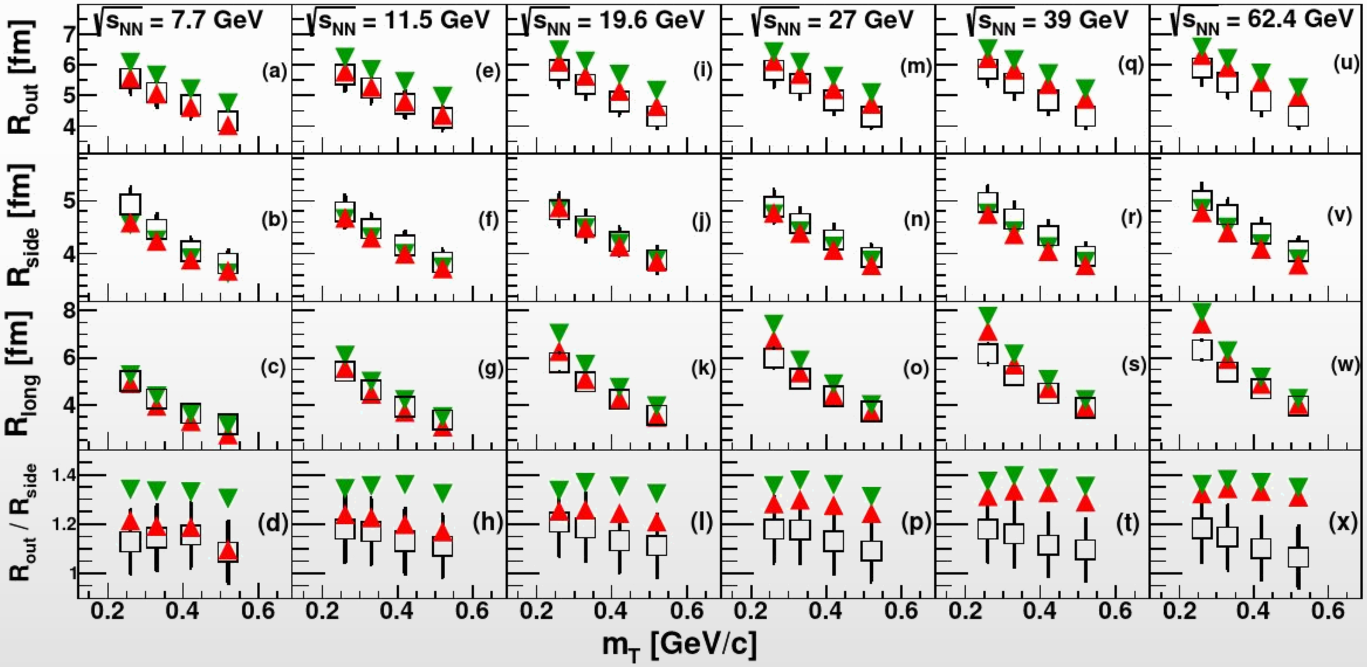

1st order phase transition

cross-over transition

- Simulations predict sensitivity of pion source size to the nature of the phase transition